IVYSPRING INTERNATIONAL PUBLISHER

International Journal of Medical Sciences

2026; 23(12): 3781-3805. doi: 10.7150/ijms.140371

Review

Recent Advances in the Pharmacology and Therapeutic Prospects of Columbianadin

Nor Hidayah Mustafa[1]✉, Juriyati Jalil[1], Haryati Ahmad Hairi[2], Yusof Kamisah[3,4]

1. Centre for Drug and Herbal Development, Faculty of Pharmacy, Universiti Kebangsaan Malaysia, Kuala Lumpur 50300, Malaysia.
2. Department of Biochemistry, Faculty of Medicine, Manipal University College Malaysia, Melaka, Malaysia.
3. Department of Pharmacology, Faculty of Medicine, Universiti Kebangsaan Malaysia, Kuala Lumpur 56000, Malaysia.
4. Cardiovascular and Pulmonary Research Group, Universiti Kebangsaan Malaysia, 43600 Bangi, Selangor, Malaysia.

✉ Corresponding author: Nor Hidayah Mustafa, Centre for Drug and Herbal Development, Faculty of Pharmacy, Universiti Kebangsaan Malaysia, Kuala Lumpur 50300, Malaysia; Email: norhidayahmustafa@ukm.edu.my.

© 2026 The Author(s). This is an open access article distributed under the Creative Commons Attribution 4.0 International Licence, subject to the Publisher's Terms of Use at https://ivyspring.com/terms.

Received: 2026.07.05; Accepted: 2026.10.29; Published: 2026.11.13

Abstract

Columbianadin, a naturally occurring coumarin derivative, has emerged as a promising bioactive compound with diverse pharmacological activities. Evidence from *in vitro* and *in vivo* studies demonstrates its anti-inflammatory, antioxidant, gastroprotective, hepatoprotective, cardioprotective, neuroprotective, bone-protective, antiplatelet, antinociceptive, cytotoxic and antiviral effects, which are mediated through the modulation of multiple signaling pathways. This review aims to comprehensively summarize the pharmacological activities and underlying molecular mechanisms of columbianadin, as well as its therapeutic potential in various disease models. It exerts its effects through the modulation of multiple key signaling pathways, including heme oxygenase-1 (HO-1)/nuclear factor kappa B (NF-κB)/mitogen-activated protein kinase (MAPK) pathway, Janus kinase 2/signal transducer and activator of transcription 3 (JAK2/STAT3) pathway, and phosphatase and tensin homolog/phosphoinositide 3-kinase/protein kinase B (PTEN/PI3K/AKT) pathway. These mechanisms highlight columbianadin as a multifunctional phytochemical with promising therapeutic potential against a wide range of pathological conditions. However, despite these encouraging preclinical findings, its clinical application remains limited due to insufficient data on its pharmacokinetics, bioavailability, and long-term safety. Further investigation is required to facilitate its translation into clinical practice.

1. Introduction

Natural products continue to serve as an important source for drug discovery, offering a vast reservoir of structurally diverse bioactive compounds with considerable therapeutic potential. Among these, coumarin derivatives have attracted substantial attention owing to their wide range of pharmacological activities. Columbianadin, a naturally occurring prenylated coumarin isolated from medicinal plants such as *Angelica pubescens* Maxim. and *Angelica decursiva* (Miq.) Franch. & Sav., has been increasingly investigated for its diverse biological properties [1]. Accumulating evidence demonstrates that columbianadin possesses multiple pharmacological activities, including anti-inflammatory [2–5], antioxidant [6, 7], hepatoprotective [4, 6, 8], cardioprotective [7, 9], antiplatelet [10, 11], antinociceptive [12], cytotoxic [13], anti-osteoporotic [14, 15], and antiviral effects [16]. Collectively, these findings highlight the therapeutic potential of columbianadin in the management of various pathological conditions, including acute reflux esophagitis, inflammatory bowel disease, rheumatoid arthritis, and neurodegenerative disorders.

Despite these promising findings, the molecular mechanisms underlying the diverse pharmacological effects of columbianadin remain insufficiently elucidated. In particular, its multi-target mechanisms of action, signaling pathways, and broader therapeutic applications warrant further investigation. A more comprehensive understanding of these aspects is

crucial for fully realizing its pharmacological and therapeutic potential. Therefore, this review aims to compile and critically evaluate the current literature on columbianadin, with particular emphasis on its chemistry, pharmacological activities, underlying molecular mechanisms, and potential as a lead compound for the development of novel therapeutic agents. To achieve this, a structured literature search was conducted using the PubMed, Scopus, and Web of Science databases from January to June 2026 to identify relevant articles published between 2011 and 2026. The search strategy combined the primary keywords "columbianadin" and "coumarin derivatives" with terms related to its biological activities and molecular mechanisms, including "pharmacological activities", "molecular mechanisms", "anti-inflammatory", "antioxidant", "gastroprotective", "hepatoprotective", "cardioprotective", "neuroprotective", "osteoprotective", "antiplatelet", "antinociceptive", "cytotoxic", and "antiviral". Original research articles reporting *in vitro*, *in vivo*, or *in silico* investigations of the pharmacological activities, cellular mechanisms, chemical structure, biosynthesis, or pharmacokinetic properties of columbianadin were considered relevant to the review. Publications providing supporting background information, including review articles, were also considered where appropriate. Duplicate records were removed before title and abstract screening, during which articles that were clearly unrelated to the scope of the review were excluded. A total of 36 relevant publications were identified, comprising 33 original research articles and three review articles. Of the original research articles, 27 investigated the pharmacological activities of columbianadin, while six addressed its chemical structure, biosynthesis, and pharmacokinetic properties. Original research articles informed the evidence synthesis, while review articles provided background information.

2. Columbianadin Structure

Columbianadin (Figure 1), chemically designated as 2-[(8*S*)-2-oxo-8,9-dihydrofuro[2,3-h]chromen-8-yl]propan-2-yl (*Z*)-2-methylbut-2-enoate, is classified as an angular dihydrofurocoumarin [17]. Structurally, it consists of a coumarin nucleus comprising a fused benzene and α-pyrone ring system, which is further fused to a five-membered dihydrofuran ring. This angular fusion pattern distinguishes columbianadin from linear furocoumarins, such as psoralen derivatives. A notable structural characteristic of columbianadin is the presence of an angelic acid ester moiety linked through an oxygen atom to the propan-2-yl substituent at C-8. This substituent, corresponding to a (*Z*)-2-methylbut-2-enoate group, contributes to the lipophilic character of the molecule and may influence its interactions with biological membranes and molecular targets. In addition, the presence of a chiral center at C-8 confers stereochemical specificity, with naturally occurring columbianadin reported to possess the (*S*) configuration when isolated from *Angelica pubescens* [17, 18].

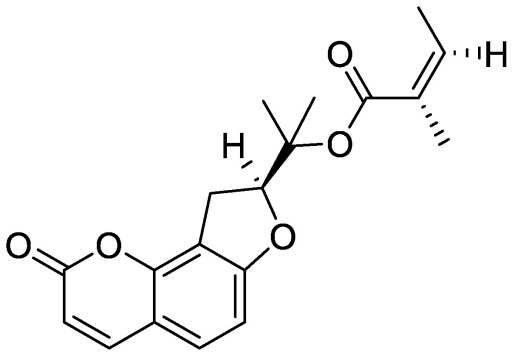


Figure 1. Molecular Structure of columbianadin.

The physicochemical properties of columbianadin are influenced by its ester linkage and lactone-containing coumarin scaffold. The ester bond is susceptible to hydrolysis, yielding angelic acid and the corresponding parent alcohol columbianetin. Furthermore, the conjugated π-electron system of the coumarin scaffold confers characteristic ultraviolet absorption, which facilitates its detection and quantification in chromatographic analyses. The relatively rigid and lipophilic architecture of the angular dihydrofurocoumarin scaffold and ester substituent may influence membrane interactions and contribute to its pharmacokinetic properties and biological activity [17, 19, 20].

3. Biosynthesis of Columbianadin

Columbianadin originates from the conversion of L-phenylalanine into the core coumarin scaffold, umbelliferone, through the phenylpropanoid pathway, involving key enzymes such as phenylalanine ammonia-lyase, cinnamate 4-hydroxylase, and p-coumaroyl-CoA 2′-hydroxylase [21]. Umbelliferone subsequently acts as a central precursor in furanocoumarin biosynthesis and undergoes prenylation at the C-8 position by prenyltransferase enzymes using dimethylallyl pyrophosphate as the prenyl donor, resulting in the formation of osthenol, an important intermediate that directs the pathway toward angular furanocoumarin biosynthesis [18]. Osthenol is then converted into (+)-columbianetin through oxidative cyclization which is

likely catalyzed by cytochrome P450 enzymes, although the precise enzymatic mechanisms remain incompletely characterized [22]. Subsequently, columbianadin is presumed to be synthesized through the esterification of columbianetin with angelic acid. Nevertheless, the specific acyltransferases responsible for this final acylation step have yet to be fully identified. The angular configuration of the furanocoumarin ring system, together with the terminal acylation, distinguishes columbianadin structurally from linear furanocoumarins.

4. Pharmacokinetics of Columbianadin

Following oral administration, columbianadin exhibits measurable plasma exposure. In healthy rats administered columbianadin orally at 25 mg/kg, it reached a maximum plasma concentration (C_{max}) of 13.33 ± 25.37 ng/mL at 3.03 ± 1.87 h (T_{max}), with an elimination half-life ($t_{1/2}$) of 5.15 ± 4.58 h. Plasma levels were detectable as early as 0.5 h post-administration. Notably, the C_{max} showed substantial variability (mean ± SD), indicating considerable inter-animal variability or uncertainty in the estimated systemic exposure, although the underlying source of this variability cannot be established from the reported summary statistics alone. In addition, columbianadin was absorbed throughout the gastrointestinal tract, with the highest absorption observed in the colon, and exhibited high permeability across Caco-2 monolayers. Interestingly, the columbianadin-containing *Angelicae pubescentis* radix extract exhibited a shorter T_{max} and $t_{1/2}$ values than purified columbianadin, suggesting that other constituents in the extract may influence its absorption and disposition [17, 23].

Systemic administration leads to rapid and widespread tissue distribution, with columbianadin detected in the heart, kidney, lung, stomach, intestine, brain, and muscle, and the highest concentration observed in the heart. Both columbianadin and its active metabolite, columbianetin, were detected in most tissues [24]. Columbianadin readily crosses the blood–brain barrier, reaching peak concentrations in the central nervous system within 30 min and exhibiting a bimodal distribution in brain tissue and cerebrospinal fluid [25]. In contrast, following oral administration of *Angelica pubescens* root extract, the liver served as the primary site of accumulation, with concentrations peaking at 6 h post-dose. Columbianadin undergoes extensive biotransformation. In rat hepatic microsomes, 13 biotransformation products were identified, primarily arising from hydroxylation, epoxidation, ester bond cleavage, and lactone ring opening. Most metabolites retained inhibitory activity against nitric oxide production, although columbianadin itself exhibited stronger activity. Overall, the available evidence indicates that columbianadin is systemically absorbed, widely distributed, capable of reaching the central nervous system, and extensively metabolized [17].

5. Biological Activities of Columbianadin

5.1 Anti-inflammatory and antioxidant activities

Inflammation and oxidative stress play central roles in the pathogenesis of numerous acute and chronic diseases [26]. Columbianadin has demonstrated significant anti-inflammatory and antioxidant activities in both *in vitro* and *in vivo* experimental models (Table 1). In lipopolysaccharide (LPS)-stimulated RAW 264.7 macrophages, columbianadin markedly suppresses the production of pro-inflammatory mediators, including tumor necrosis factor-α (TNF-α), interleukin (IL)-6, IL-1β, inducible nitric oxide synthase (iNOS), prostaglandin E_2 (PGE_2), cyclooxygenase-2 (COX-2), and nitric oxide, while simultaneously reducing hydroxyl radical generation [4, 5, 27]. These anti-inflammatory effects are mechanistically associated with the upregulation of the cytoprotective enzyme heme oxygenase-1 (HO-1) and the inhibition of inhibitor of κB (IκB) kinase activity, leading to the suppression of nuclear factor-κB (NF-κB) signaling [4].

In addition to its effects in macrophages, post-treatment of THP-1 human monocytic leukemia cells with columbianadin (30–100 μg/mL) significantly downregulated the expression of TNF-α, IL-1β, NF-κB p65, monocyte chemoattractant protein-1 (MCP-1), nucleotide-binding oligomerization domain-containing protein 1 (NOD1), and receptor-interacting protein kinase 2 (RIP2), accompanied by a reduction in apoptotic cell death [3]. NOD1 functions as an intracellular pattern-recognition receptor that, upon activation, recruits receptor-interacting protein kinase 2 (RIP2) to initiate downstream NF-κB and mitogen-activated protein kinase (MAPK) signaling pathways, thereby amplifying inflammatory responses [28]. The observed suppression of NOD1/RIP2 signaling by columbianadin therefore suggests an additional mechanism through which the compound attenuates inflammatory signaling cascades (Figure 2).

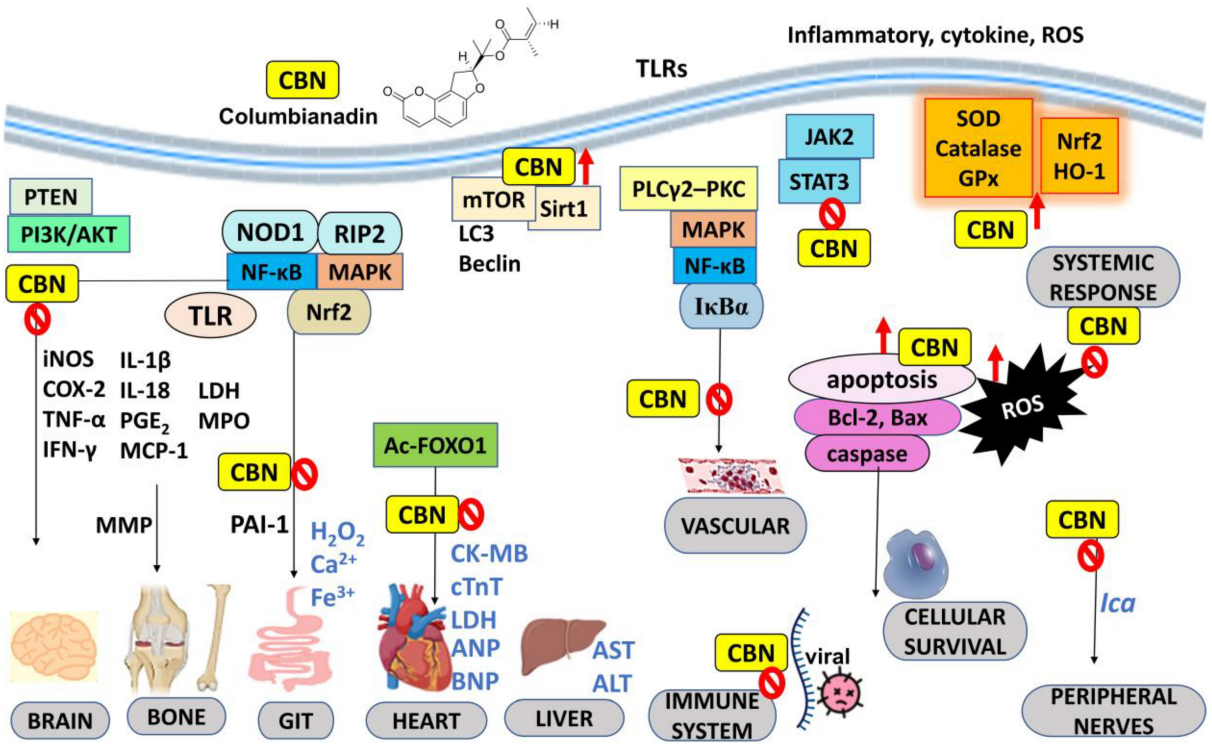


Figure 2. Schematic representation of the molecular pathways and therapeutic targets modulated by columbianadin. Abbreviation: Ac-FOXO1: acetylated Forkhead box O1; AKT: protein kinase B; ALT: alanine aminotransferase; ANP: atrial natriuretic peptide; AST: aspartate aminotransferase; Bcl-2: B-cell lymphoma 2; Bax: Bcl-2-associated X protein BNP: brain natriuretic peptide; Ca^{2+}: calcium; CBN: columbianadin; CK-MB: creatine kinase-MB; COX-2: cyclooxygenase; cTnT: cardiac troponin T; Fe^{3+}: iron; GIT: gastrointestinal tract; GPx: glutathione peroxidase; H_2O_2: hydrogen peroxide; HO-1: heme oxygenase-1; *Ica*: voltage-gated calcium currents; IκBα: nuclear factor of κB inhibitor α; IFN-γ: interferon-γ; IL: interleukin; iNOS: inducible nitric oxide synthase; JAK2: janus kinase 2; LC3: microtubule-associated protein 1A/1B-light chain 3; LDH: lactate dehydrogenase; MAPK: mitogen-activated protein kinase; MCP-1: monocyte chemoattractant protein-1; MMP: matrix metalloproteinase; MPO: myeloperoxidase; mTOR: mammalian target of rapamycin; NF-κB: nuclear factor kappa-light-chain-enhancer of activated B cells; NOD1: nucleotide-binding oligomerization domain-containing protein 1; Nrf2: nuclear factor erythroid 2-related factor 2; PAI-1: plasminogen activator inhibitor-1; PGE_2: prostaglandin E_2; PI3K: phosphoinositide 3-kinase; PKC: protein kinase C; PLCγ2: Phospholipase Cγ2; PTEN: phosphatase and tensin homolog; RIP2: receptor-interacting protein 2; ROS: reactive oxygen species; Sirt1: sirtuin 1; SOD: superoxide dismutase; STAT3: signal transducer and activator of transcription 3; TLRs: toll-like receptors; TNF-α: tumor necrosis factor α. Certain icons were created with BioRender.com.

Furthermore, columbianadin has been shown to modulate MAPK signaling pathways, including extracellular signal-regulated kinase (ERK), p38, and c-Jun N-terminal kinase (JNK), thereby suppressing downstream inflammatory transcriptional activity while enhancing endogenous antioxidant defenses, such as superoxide dismutase (SOD), catalase, and glutathione peroxidase [4, 6]. However, notable discrepancies exist regarding the effects of columbianadin on p38 MAPK phosphorylation across different experimental models. Jayakumar et al. (2021) reported that p38 MAPK phosphorylation remained unaffected in LPS-stimulated RAW 264.7 macrophages following a brief 20-min pretreatment with columbianadin (20-40 μM) [4]. In contrast, Ma et al. (2024) observed significant suppression of p38 MAPK activation in a D-galactose-induced aging mouse model following chronic oral administration of columbianadin (200-800 mg/kg) for 8 weeks [6]. These apparently conflicting findings suggest that the effects of columbianadin on p38 MAPK signaling may be context-dependent and influenced by differences in experimental models and cell types, treatment duration, and dose. The discrepancy may partly reflect differences between acute *in vitro* exposure and chronic *in vivo* administration, as well as variations in the upstream regulatory mechanisms engaged under these experimental conditions, including MAPK kinases such as MAPK kinase 3/6 (MKK3/6). Nevertheless, the precise mechanisms underlying these differential effects remain unclear and warrant further investigation.

Consistent with these *in vitro* findings, columbianadin also attenuates inflammatory responses *in vivo*. In an LPS-induced acute lung injury mouse model, columbianadin isolated from the roots of *Angelica decursiva* reduced inflammatory cell infiltration into lung tissues, including alveolar macrophages, dendritic cells, interstitial macrophages, and neutrophils. It also decreased alveolar wall thickness and inflammatory changes in bronchoalveolar lavage fluid, collectively demonstrating its protective effects against pulmonary inflammation [29]. These findings further suggest that the reduction in inflammatory cell numbers in bronchoalveolar lavage fluid observed

following treatment with the *Angelica decursiva* extract in the same study may be partly attributable to the columbianadin present in the extract [29]. Similarly, in a D-galactose-induced aging mouse model, chronic administration of columbianadin (200–800 mg/kg) significantly reduced oxidative stress and inflammatory markers by enhancing endogenous antioxidant enzyme activities while suppressing the activation of Janus kinase 2/signal transducer and activator of transcription 3 (JAK2/STAT3), NF-κB p65, and p38 signaling pathways [6]. Although these findings suggest that columbianadin possesses antioxidant properties, its antioxidative effects have not been comprehensively characterized, as the study primarily focused on its anti-inflammatory and anti-aging activities rather than providing detailed mechanistic insights into its modulation of oxidative stress.

Despite the reported pharmacokinetic findings, a substantial translational gap exists between systemic exposure to columbianadin following oral administration and the concentrations used in some in vitro studies. In healthy rats, oral administration of columbianadin at 25 mg/kg resulted in C_{max} of 13.33 ± 25.37 ng/mL, equivalent to approximately 0.041 μM based on its molecular weight of 328.36 g/mol. Notably, the reported C_{max} exhibited substantial variability, and unbound plasma concentrations have not been established. In contrast, many *in vitro* studies reported biological effects at concentrations substantially higher than 0.041 μM (Table 1), in some cases exceeding the estimated total plasma C_{max} by several hundred-fold. This discrepancy raises questions regarding the translational relevance of the observed effects at these concentrations.

However, this comparison should be interpreted cautiously because the pharmacokinetic data were obtained at a specific oral dose in healthy rats and do not establish the systemic or tissue exposure achieved in other experimental models. Other *in vivo* studies have employed substantially higher doses, including 200–800 mg/kg in chronic treatment model [6]; however, the corresponding plasma exposures remain unclear in the absence of pharmacokinetic data at these doses. Furthermore, differences in protein binding, tissue distribution, intracellular accumulation, active metabolites, treatment duration, and disease state may influence the relationship between plasma exposure and pharmacological response. Thus, the available evidence neither establishes that the high concentrations used *in vitro* are achievable in target tissues following oral administration nor demonstrates that the observed effects necessarily arise from nonspecific off-target activity. Future studies should establish concentration–response relationships across a range of exposures, characterize the pharmacokinetics, plasma protein binding, tissue distribution, and potential activity of columbianadin metabolites, and integrate pharmacokinetic and pharmacodynamic data to determine whether the reported mechanisms can be reproduced at pharmacologically relevant exposures. Until such evidence becomes available, the *in vitro* findings should be interpreted as evidence of biological activity under the experimental conditions tested rather than confirmation of therapeutic efficacy at achievable *in vivo* exposures.

Collectively, these findings highlight the therapeutic potential of columbianadin through its broad anti-inflammatory effects across multiple experimental models, with preliminary evidence also suggesting antioxidative activity. These protective effects appear to be mediated through the coordinated modulation of several key signaling pathways, particularly the HO-1/NF-κB/MAPK and JAK2/STAT3 pathways, which play critical roles in the regulation of inflammation and oxidative stress. Nevertheless, further studies are needed to comprehensively elucidate the antioxidant and anti-inflammatory mechanisms of columbianadin. Future investigations should include detailed evaluations of mitochondrial oxidative status, glutathione homeostasis, nuclear factor erythroid 2-related factor 2 (Nrf2)-mediated antioxidant signaling, and the expression of downstream antioxidant enzymes to better define its role in oxidative stress regulation. In addition, assessment of inflammation-related parameters, including NOD-like receptor family pyrin domain containing 3 (NLRP3) inflammasome activation, macrophage polarization, pro-inflammatory cytokine profiles, and immune cell infiltration, would provide further insight into the immunomodulatory effects of columbianadin under inflammatory conditions.

5.2 Gastroprotective effects

Excessive oxidative stress and dysregulated inflammatory responses can disrupt mucosal homeostasis, leading to epithelial injury and the development of gastrointestinal disorders such as reflux esophagitis and inflammatory bowel disease [31]. Columbianadin has been reported to exert gastroprotective effects by protecting the esophageal and intestinal mucosa through coordinated antioxidant, anti-inflammatory, barrier-protective, and anti-apoptotic mechanisms. In Swiss albino Wistar rats, reflux esophagitis was induced by dual ligation of the pylorus and the forestomach–corpus junction, and oral administration of columbianadin (25, 50, and 100 mg/kg) dose-dependently reduced

gastric acid secretion volume and total acidity while increasing gastric pH [5]. These protective effects were closely associated with attenuation of oxidative stress, as evidenced by reduced malondialdehyde (MDA) and hydrogen peroxide levels, both of which are established markers of oxidative damage associated with reactive oxygen species (ROS).

Table 1. Anti-inflammatory and antioxidant activities of columbianadin and columbianadin-containing extracts

Model	Dose	Findings	Reference
LPS-stimulated THP-1 cells	Pretreated 20 μM for 1 h (purified columbianadin)	↓ TNF-α	[8]
LPS-stimulated RAW264.7 cells	IC_{50} value of 30.32 μM (purified columbianadin)	↓ NO levels	[27]
IL-1β-stimulated lung epithelial cells (A549)	Concurrent treatment 100 μM for 4 h (purified columbianadin)	↓ IL-6	[29]
LPS-stimulated alveolar macrophages (MH-S)	Concurrent treatment 50, 100 μM for 24 h (purified columbianadin)	↓ NO levels ↓ iNOS protein expression	[29]
LPS-induced acute lung injury in mice	Pretreatment with 400 mg/kg columbianadin-containing *Angelica decursiva* root extract, 1 h before induction, oral	↓ number of cells in bronchoalveolar lavage fluid	[29]
LPS-induced acute lung injury in mice	Pretreatment 20 and 60 mg/kg, 1 h before induction, oral (purified columbianadin)	↓ numbers of alveolar macrophages in broncho alveolar lavage fluid ↓ number of dendritic cells in broncho alveolar lavage fluid ↓ interstitial macrophage in broncho alveolar lavage fluid ↓ neutrophil in broncho alveolar lavage fluid ↓ alveolar wall thickness	[29]
LPS-stimulated RAW 264.7 cell	Pre-treatment 0.5-50 μM, for 2h (purified columbianadin)	↓ NO levels ↓ MCP-1 ↔ TNF-α ↔ IL-6	[2]
LPS-stimulated THP-1 cells	Post-treatment 30-100 μg/mL (91.36 -304.54 μM) for 24 h (purified columbianadin)	↓ TNF-α ↓ IL-1β ↓ MCP-1 ↓ NOD1 mRNA expression ↓ RIP2 mRNA expression ↓ NF-κB p65 mRNA expression ↓ apoptosis cells (%)	[3]
LPS-stimulated RAW 264.7 cell	Pretreated 20 and 40 μM for 20 min (purified columbianadin)	↓ TNF-α protein expression ↓ IL-1β protein expression ↓ iNOS protein expression ↓ NO levels ↓ hydroxyl radical ↑ HO-1 protein expression ↓ p-ERK protein expression ↓ p-JNK protein expression ↔ p-p38 protein expression ↑ IκB protein expression ↓ p-p65 protein expression ↓ NF-κB p65 nuclear translocation	[4]
LPS-stimulated RAW264.7	Concurrent treatment 25, 50, 100 μg/mL for 24 h with a columbianadin-containing combined extract of *Angelicae pubescentis* radix and *Notopterygii* rhizoma et radix	↓ NO levels	[30]
LPS-stimulated RAW 264.7 cell	Concurrent treatment 20, 40 and 80 μM for 24h (purified columbianadin)	↓ TNF-α ↓ IL-6 ↓ IL-1β ↓ iNOS ↓ PGE_2 ↓ COX-2 ↓ nitric oxide	[5]
D-galactose-induced aging in mice	Concurrent treatment 200, 400 and 800 mg/kg in corn oil for 8 weeks (purified columbianadin)	↓ MDA ↑ SOD ↑ catalase ↑ GSH-Px ↓ TNF-α ↓ IL-1β ↓ IL-6 ↓ edema ↓ inflammatory cell infiltration ↓ p-JAK2/JAK2 ↓ p-STAT3/STAT3 ↓ p-p65/p65 ↓ p-p38/p38	[6]

Abbreviation: COX-2: cyclooxygenase-2; GSH-Px: glutathione peroxidase; MCP-1: monocyte chemoattractant protein-1; IL: interleukin; IκB: inhibitor of κB; iNOS: inducible nitric oxide synthase; JAK: janus kinase 2; LPS: lipopolysaccharide; MCP: monocyte chemoattractant protein-1; MDA: malondialdehyde; NO: nitric oxide; NOD: nucleotide-binding oligomerization domain; NF-κB: nuclear factor-κB; p-ERK: phosphorylated extracellular regulated protein kinases; PGE_2: prostaglandin E_2; p-JAK2: phosphorylated janus kinase 2; p-JNK: phosphorylated c-Jun N-terminal kinase; p-p38: phosphorylated p38; p-p65: phosphorylated p65; RIP2: receptor-interacting protein 2; SOD: superoxide dismutase; p-STAT3: phosphorylated signal transducer and activator of transcription 3; THP-1: the human monocytic leukemia cell line; TNF-α: tumor necrosis factor alpha; ↓: decreased; ↑: increased; ↔: no changes.

Columbianadin also decreases free iron accumulation and intracellular calcium overload, both of which can exacerbate oxidative injury. Excess free iron catalyzes the Fenton reaction, leading to the generation of highly reactive hydroxyl radicals that intensify lipid peroxidation and cellular damage, whereas intracellular calcium overload promotes mitochondrial dysfunction, excessive ROS production, and activation of calcium-dependent degradative enzymes [32, 33]. By limiting free iron accumulation and maintaining calcium homeostasis, columbianadin may prevent the secondary cascade of oxidative and biochemical damage following the initial reflux insult. Furthermore, columbianadin enhances endogenous antioxidant defense systems by increasing the activities of superoxide dismutase (SOD), catalase, and glutathione peroxidase (GPx), while also elevating plasma free radical-scavenging activity and sulfhydryl group levels (Table 2). Collectively, these effects may contribute to free radical neutralization, preservation of redox homeostasis, and protection of gastric mucosal tissues against reflux-induced injury [5].

Beyond its antioxidant properties, columbianadin also suppresses the expression of multiple pro-inflammatory mediators, including TNF-α, IL-1β, IL-6, IL-17, COX-2, iNOS, PGE2, and MCP-1, while simultaneously increasing the anti-inflammatory cytokine IL-10 in reflux esophagitis. These protective effects are associated with inhibition of plasminogen activator inhibitor-1 (PAI-1) expression and suppression of NF-κB signaling. Together, these findings suggest that columbianadin modulates both inflammatory activation and fibrinolytic imbalance. Such modulation may contribute to the attenuation of inflammatory injury and enhancement of mucosal repair processes in reflux-associated esophageal damage [5].

The gastroprotective effects of columbianadin have also been demonstrated in inflammatory bowel disease models. In dextran sulfate sodium-induced ulcerative colitis in Swiss albino Wistar rats, concurrent oral administration of columbianadin (5, 10, and 15 mg/kg) for 7 days significantly ameliorated disease severity, as evidenced by reductions in disease activity index and improvements in colon length, body weight, lactate dehydrogenase levels, and daily food and water intake [34]. In ulcerative colitis, elevated interferon-γ (IFN-γ) contributes to disease progression by activating macrophages and enhancing the release of pro-inflammatory cytokines, thereby amplifying intestinal inflammation [35]. Columbianadin suppressed inflammatory mediators including IFN-γ, nitric oxide, iNOS, COX-2, PGE_2, TNF-α, MCP-1, and several interleukins that are typically upregulated during intestinal inflammation. Concurrently, it enhanced intracellular antioxidant defense systems, including catalase, SOD, and glutathione-related enzymes, while reducing MDA levels and myeloperoxidase (MPO) activity. MPO is a heme-containing enzyme abundantly released by activated neutrophils that catalyzes the generation of potent antimicrobial oxidants during inflammatory responses [36]. The reduction in MPO activity by columbianadin suggests attenuation of both neutrophil infiltration and oxidant-mediated injury in colonic tissues.

Moreover, columbianadin preserves intestinal barrier integrity and modulates apoptosis-related signaling pathways. It suppresses the expression of apoptosis-associated speck-like protein containing a CARD (ASC), a key inflammasome adaptor involved in the amplification of inflammatory signaling. Columbianadin also upregulates the tight junction proteins occludin and zonula occludens-1 (ZO-1), both of which are essential for maintaining epithelial barrier integrity in colonic tissues [37, 38]. Furthermore, columbianadin regulates apoptotic signaling by upregulating B-cell lymphoma 2 (Bcl-2) expression and downregulating Bcl-2-associated X protein (Bax) expression, thereby increasing the Bcl-2/Bax ratio and promoting epithelial cell survival. Its anti-apoptotic effect is further supported by reduced caspase-1 and activated caspase-3 (A-caspase-3) levels, suggesting suppression of inflammasome-associated inflammatory signaling and the execution phase of apoptosis in colonic tissues [34].

Recent advances have further expanded the therapeutic potential of columbianadin through nanozyme-based drug delivery systems designed to enhance its stability, bioavailability, and targeted accumulation in inflamed colonic tissues. This columbianadin-based nanoformulation exhibits high biocompatibility in NCM460 normal colon cells and restores intestinal mucosal integrity while suppressing pro-inflammatory mediators, including TNF-α and IL-6, in dextran sulfate sodium-induced inflammatory bowel disease in mice [39]. Mechanistically, the gastroprotective effects of columbianadin are associated with activation of the HO-1/Nrf2 antioxidant pathway and suppression of toll-like receptor 4 (TLR4)/NF-κB, p38 MAPK, and transforming growth factor-β (TGF-β) signaling pathways. These effects enhance endogenous antioxidant defenses while attenuating inflammatory signaling cascades in gastrointestinal tissues. Further advances include encapsulating MXene/columbianadin in gelatin methacryloyl hydrogel microspheres to produce MXene/columbianadin@GelMA (MCG). Although unencapsulated MXene/columbianadin exhibits ROS-

scavenging and oxygen-generation activities, its *in vivo* efficacy may be limited by rapid gastrointestinal clearance and insufficient colonic retention. GelMA encapsulation is designed to improve gastrointestinal protection, local retention, and ROS-responsive release at inflamed colonic sites. In dextran sulfate sodium-induced colitis in mice, MCG demonstrated superior therapeutic effects compared with unencapsulated MXene/CBN, including reduced disease activity index scores and tissue edema, improved colon length and mucosal architecture, restored goblet cells, and decreased intestinal permeability. These findings suggest that GelMA encapsulation enhances the delivery and therapeutic efficacy of MXene/CBN, highlighting its potential for inflammatory bowel disease treatment [39]. However, further studies are needed to establish its long-term safety, pharmacokinetics, and clinical applicability.

Table 2. Gastroprotective effects of columbianadin

Model	Dose	Findings	Reference
Ligation of pylorus and fore stomach and corpus junction-induced reflux esophagitis in Swiss albino Wistar rats	Pretreatment 25, 50 and 100 mg/kg (1 h before induction), oral	↓ gastric secretion volume ↓ total acidity ↑ gastric pH ↓ H_2O_2 ↓ free iron ↓ calcium ↑ plasma scavenging activity (%) ↑ sulfhydryl group ↓ MDA ↑ GSH ↑ SOD ↑ catalase ↑ GPx ↓ TNF-α ↓ IL-6 ↓ IL-1β ↑ IL-10 ↓ IL-17 ↓ MCP-1 ↓ PGE_2 ↓ COX-2 ↓ iNOS ↓ NF-κB ↓ TNF-α mRNA expression ↓ IL-6 mRNA expression ↓ IL-1β mRNA expression ↓ PAI-1 mRNA expression	[5]
Dextran sulfate sodium-induced ulcerative colitis in Swiss albino Wistar rats	Concurrent treatment 5, 10 and 15 mg/kg, oral for 7 days	↑ body weight ↑ colon length ↓ spleen index ↓ disease activity index ↑ average daily food intake ↑ average daily water intake ↓ LDH ↓ MPO ↑ catalase ↑ SOD ↑ GR ↑ GPx ↓ MDA ↓ NO ↑ HO-1 ↑ nrf-2 ↓ IL-1 ↓ IL-1β ↓ IL-1β mRNA expression ↓ IL-6 ↓ IL-6 mRNA expression ↑ IL-10 ↓ IL-17 ↓ IL-18 ↓ TNF-α ↓ TNF-α mRNA expression ↓ PGE2 ↓ COX-2 ↓ iNOS ↓ NF-κB ↓ TGF-β ↓ Bax ↓ Bax mRNA expression ↑ Bcl-2 ↑ Bcl-2 mRNA expression ↑ Bcl-2/Bax	[34]

Model	Dose	Findings	Reference
		↓ caspase-1 ↓ activated-caspase-3 ↓ MCP-1 ↓ MCP-1 mRNA expression ↓ IFN-γ mRNA expression ↓ IL-8 mRNA expression ↓ NF-κB mRNA expression ↓ TLR4 mRNA expression ↓ p38 mRNA expression ↓ ASC mRNA expression ↑ ZO-1 mRNA expression ↑ Ocln mRNA expression	
Dextran sulfate sodium-induced inflammatory bowel disease in mice	MXene/columbianadin (0.1 mg/kg) and MCG (0.1 mg/kg), oral on days 1, 3, 5, and 7	Both: ↓ disease activity index ↑ colon length ↑ mucosal barrier integrity ↓ body weight loss ↓ TNF-α ↓ IL-6	[39]
Human colon mucosal epithelial cells (NCM460)	MXene/columbianadin (26.1 μg/mL) and MCG (200 μg/mL)	Both: ↓ reactive oxygen species ↑ intracellular oxygen generation	[39]

Abbreviation: ASC: apoptosis-associated speck-like protein containing a CARD; COX-2: cyclooxygenase-2; GPx: glutathione peroxidase; GR: glutathione reductase; iNOS: inducible nitric oxide synthase; SOD: superoxide dismutase; TGF-β: transforming growth factor-β; TNF-α: tumor necrosis factor-α; IFN-γ: interferon-γ; IL: interleukin; LDH: lactate dehydrogenase; MCP-1: monocyte chemoattractant protein-1; MDA: malondialdehyde; MCG, MXene/columbianadin@ gelatin methacryloyl hydrogel; MPO: myeloperoxidase; NF-κB: nuclear factor-κB; NO: nitric oxide; Ocln: occludin; PAI-1: plasminogen activator inhibitor-1; PGE_2: prostaglandin E_2; ZO-1: zonula occludens-1; ↓: decreased; ↑: increased; ↔: no changes.

5.3 Neuroprotective effects

Following spinal cord injury, microglia predominantly polarize toward the M1 (pro-inflammatory) phenotype, leading to the release of cytokines that contribute to neuronal damage. Columbianadin attenuates neuroinflammation by inhibiting M1 microglial polarization and suppressing amoeboid morphological transformation under LPS-induced inflammatory conditions in BV2 microglia. These effects are associated with reduced expression of iNOS, COX-2, TNF-α, IL-1β, phosphorylated phosphoinositide 3-kinase (p-PI3K), and phosphorylated protein kinase B (p-AKT) (Table 3) [40]. To further examine the effects of activated microglia on neuronal survival, ventral spinal cord 4.1 (VSC4.1) motor neurons were exposed to conditioned medium collected from BV2 microglia. This approach enabled the assessment of neuronal responses to soluble factors released by activated microglia without direct cell-to-cell contact. Exposure to conditioned medium from LPS-stimulated microglia reduced the expression of the anti-apoptotic protein B-cell lymphoma-extra large (Bcl-xL) and induced neuronal apoptosis. In contrast, conditioned medium from columbianadin-pretreated, LPS-stimulated microglia restored Bcl-xL expression and attenuated apoptosis in VSC4.1 motor neurons. Consistent with these *in vitro* findings, columbianadin treatment (15 mg/kg for 7 days) in a female Sprague Dawley rat model of spinal cord injury improved motor function recovery, reduced cavity formation at the injury site, decreased the number of CD68-positive cells, suppressed the expression of iNOS, COX-2, p-PI3K, and p-AKT, and increased phosphatase and tensin homolog (PTEN) expression. PTEN is a negative regulator of PI3K/AKT signaling and plays an important role in controlling microglial inflammatory activation. Columbianadin was reported to enhance PTEN stability by suppressing its ubiquitination and degradation, thereby promoting PTEN-mediated inhibition of PI3K/AKT signaling. This mechanism may contribute to the suppression of M1 microglial polarization, reduction of neuroinflammation, and improvement of functional recovery following spinal cord injury [40].

Overall, these findings highlight columbianadin as a promising neuroprotective agent for mitigating neuroinflammation and promoting functional recovery following spinal cord injury through PTEN-mediated inhibition of the PI3K/AKT signaling pathway. Further studies are warranted to validate the neuroprotective effects of columbianadin in clinically relevant spinal cord injury models, further elucidate its interactions with PTEN and downstream signaling components, and evaluate its pharmacokinetic properties, safety, and delivery strategies to facilitate future clinical translation.

5.4 Hepatoprotective activity

Columbianadin exhibits hepatoprotective effects supported by findings from several experimental studies, which are primarily attributed to its antioxidant properties that reduce oxidative stress and lipid peroxidation in hepatic tissues (Table 4) [4, 6]. Intraperitoneal administration of columbianadin (10 mg/kg) for 7 consecutive days significantly reduced serum markers of liver injury, including aspartate aminotransferase (AST) and alanine aminotransferase (ALT), in carbon tetrachloride-induced hepatotoxicity in Sprague–Dawley rats [8]. Similarly, pretreatment

with columbianadin (20 mg/kg, intraperitoneal) 2 h before induction decreased ALT and AST levels in an LPS-induced acute liver inflammation model in C57BL/6 mice [4]. Histopathological analysis further demonstrated that LPS-induced hepatic injury, characterized by collagen deposition, increased elastic fiber formation, thickening of the portal vein, and proliferation of reticular fibers, was markedly attenuated following columbianadin treatment [4]. In a D-galactose–induced liver injury model, columbianadin-treated groups (200, 400, and 800 mg/kg) showed reduced body weight loss and attenuation of the decline in liver index, along with decreased ALT and AST levels compared with untreated animals [6]. Hepatic architecture was largely restored toward normal morphology, with reduced Suzuki scores, indicating histological improvement comparable to that observed with vitamin E treatment (Table 4) [6].

Collectively, histological analyses corroborated the biochemical findings, demonstrating that columbianadin preserves hepatic structural integrity, which may contribute to reduced hepatocyte membrane damage and the release of ALT and AST into the systemic circulation. These findings support the hepatoprotective potential of columbianadin. Nevertheless, further studies are required to elucidate the precise molecular mechanisms underlying columbianadin-mediated hepatoprotection, particularly its regulatory effects on oxidative stress, inflammatory responses, and fibrotic pathways. Investigation using chronic and clinically relevant liver disease models, together with comprehensive assessments of pharmacokinetics, bioavailability, and long-term safety, will be essential to determine its therapeutic applicability and facilitate future clinical translation.

5.5 Cardioprotective effects

The cardioprotective effects of columbianadin have been demonstrated in experimental models of cardiac injury, including drug-induced cardiotoxicity and left anterior descending coronary artery ligation-induced acute myocardial infarction in mice. In a doxorubicin-induced cardiotoxicity model in C57BL/6 mice, intraperitoneal administration of columbianadin (10 mg/kg) improved cardiac function and attenuated myocardial injury [7]. This was evidenced by reduced mRNA expression of atrial natriuretic peptide and brain natriuretic peptide, established markers of cardiac wall stress and heart failure, as well as decreased serum levels of creatine kinase-MB, cardiac troponin T, and lactate dehydrogenase. Echocardiographic assessment further showed improved cardiac performance, including increased ejection fraction and fractional shortening, along with enhanced left ventricular contractility, as reflected by an elevated maximum rate of rise of left ventricular pressure over time (+dP/dt). Mechanistically, these cardioprotective effects were associated with activation of the Forkhead box O1–Sirtuin 1 (FOXO1–SIRT1) signaling axis, as indicated by upregulation of SIRT1 expression and reduced FOXO1 acetylation. SIRT1-mediated deacetylation enhances FOXO1 transcriptional activity, promoting antioxidant defenses through upregulation of Nrf2 and heme oxygenase-1, while facilitating adaptive autophagy and suppressing apoptosis. This is supported by reduced numbers of TUNEL-positive cells, an increased Bcl-2/Bax ratio, and decreased cleaved caspase-3 expression [7, 42].

Table 3. Neuroprotective effects of columbianadin

Model	Dose	Findings	Reference
LPS-induced inflammation in BV2 microglia cells	Pre-treatment 12.5, 25 and 50 μM for 12h	↓ iNOS mRNA expression ↓ iNOS protein expression ↓ iNOS fluorescence intensity ↓ COX-2 mRNA expression ↓ COX-2 protein expression ↓ TNF-α mRNA expression ↓ IL-1β mRNA expression ↓ p-PI3K/PI3K protein expression ↓ p-AKT/AKT protein expression	[40]
VSC4.1 motor neurons exposed to LPS-stimulated microglial conditioned medium	Pre-treatment 12.5, 25 and 50 μM for 12h	↑ Bcl-xL protein expression ↓ neuronal apoptosis	[40]
Spinal cord injury in female Sprague Dawley rats	Post-treatment 15 mg/kg for 7 days, i.p.	↑ Hindlimbs motor function ↓ longitudinal cavity area in spinal cord injury region ↓ CD68-positive microglia (M1) ↓ iNOS protein expression ↓ COX-2 protein expression ↓ p-PI3K/PI3K protein expression ↓ p-AKT/AKT protein expression ↑ PTEN protein expression ↑ neural regeneration post-spinal cord injury	[40]

Abbreviation: Akt: protein kinase-B; Bcl-xL: B-cell lymphoma-extra large; COX-2: cyclooxygenase-2; iNOS: inducible nitric oxide synthase; IL: interleukin; LPS:

lipopolysaccharide; PI3K: phosphatidylinositol 3-kinase; PTEN: phosphatase and tensin homolog; TNF-α: tumor necrosis factor-α; VSC4.1; ventral spinal cord 4.1; ↓: decreased; ↑: increased; ↔: no changes.

Table 4. Hepatoprotective effects of columbianadin

Model	Dose	Findings	Reference
CCl_4-induced hepatotoxicity in Sprague–Dawley rats	10 mg/kg, i.p. daily for 7 days	↓ AST ↓ ALT	[8]
LPS-induced acute liver inflammation in C57BL/6 mice	Pretreated 20 mg/kg, i.p. for 2 h	↓ AST ↓ ALT ↓ collagens and elastic fibers in liver tissues ↓ reticular fibers between the sinusoids and the plates of hepatocytes ↓ thickening of the portal vein in the livers	[4]
Collagen-induced arthritis in male DBA/1 mice	Post-treatment, 20 mg/kg orally for 3 weeks	↓ AST ↓ ALT	[41]
D-galactose-induced-aging in mice	Concurrent treatment 200, 400 and 800 mg/kg in corn oil for 8 weeks	↓ AST ↓ ALT ↓ edema ↓ suzuki score	[6]

Abbreviation: AST: aspartate aminotransferase; ALT: alanine aminotransferase; CCl_4: carbon tetrachloride; LPS: lipopolysaccharide; i.p: intraperitoneal; ↓: decreased; ↑: increased; ↔: no changes.

In another study, post-treatment with columbianadin (10, 20 and 40 mg/kg, orally for 28 days) significantly ameliorated cardiac injury in C57BL/6 mice with doxorubicin-induced cardiotoxicity. Treated mice exhibited improved cardiac function, as indicated by increased left ventricular ejection fraction and fractional shortening, along with reduced left ventricular internal dimensions at end-diastole and end-systole [9]. These findings were consistent with attenuation of myocardial and ultrastructural damage, as evidenced by decreased lactate dehydrogenase levels, reduced cardiac fibrosis and collagen fiber deposition, restoration of mitochondrial morphology, and a reduced number of autophagosomes. Myocardial tissue relies on autophagy to maintain intracellular homeostasis, facilitate organelle turnover, and sustain energy balance under stress conditions [43]. In this study, columbianadin suppressed excessive autophagy by downregulating microtubule-associated protein 1A/1B-light chain 3 (LC3), Beclin-1, and autophagy-related protein 5 (Atg5), while upregulating p62 expression in cardiac tissue. This effect was associated with modulation of the phosphatidylinositol 3-kinase (PI3K)/protein kinase B (AKT)/mammalian target of rapamycin (mTOR) signaling pathway, as evidenced by increased p-PI3K/PI3K, p-AKT/AKT, and p-mTOR/mTOR ratios (Table 5).

Consistent with these findings, concurrent treatment with columbianadin (1 and 10 μM) in hypoxia-treated H9c2 cardiomyocytes restored cell viability, reduced ROS production, improved mitochondrial respiratory function, and increased mitochondrial membrane potential, indicating enhanced mitochondrial integrity and cellular survival under hypoxic stress. In LC3 dual-fluorescent adenovirus-transfected H9c2 cells, autophagic flux increased under hypoxia but was subsequently inhibited following columbianadin treatment, suggesting that its cardioprotective effects may be mediated, at least in part, through regulation of autophagy [9].

Taken together, the cardioprotective effects of columbianadin appear to involve coordinated modulation of the FOXO1–SIRT1 and PI3K/AKT/mTOR signaling pathways, which collectively regulate oxidative stress, apoptosis, and autophagy, thereby contributing to the preservation of myocardial structure and function [7, 9].

5.6 Bone-protective effect

Rheumatoid arthritis is a chronic autoimmune inflammatory disease characterized by aberrant immune-mediated attacks on the synovial lining of the joints, resulting in persistent inflammation, pain, cartilage degradation, and progressive bone destruction [44]. Despite advances in therapeutic strategies, no definitive cure is currently available. Clinical management primarily relies on nonsteroidal anti-inflammatory drugs (NSAIDs), glucocorticoids, and disease-modifying antirheumatic drugs (DMARDs), such as methotrexate, which primarily provide symptomatic relief and slow disease progression without eliminating the underlying disease [45].

Table 5. Cardioprotective effects of columbianadin

Model	Dose	Findings	Reference
Doxorubicin-induced cardiotoxicity in C57BL/6 mice	Post-treatment 10 mg/kg/day, i.p. for 4 weeks	↑ HW/TL ↓ ANP mRNA expression ↓ BNP mRNA expression ↑ EF (%) ↑ FS (%) ↑ +d*P*/dt ↓ CK-MB ↓ cTnT ↓ LDH ↓ ROS levels ↑ Nrf2 protein expression ↑ HO-1 protein expression ↓ MDA ↑ catalase ↓ TUNEL-positive cells (%) ↑ Bcl-2 protein expression ↓ C-caspase3 protein expression ↓ Bax protein expression ↑ Sirt1 protein expression ↑ Sirt1 deacetylation activity ↓ Ac-FOXO1/FOXO1 protein expression	[7]
Left anterior descending coronary artery ligation induced acute myocardial infarction in mice	Post-treatment 10, 20 and 40 mg/kg, oral for 28 days	↑ LVEF ↑ FS ↓ LVIDd ↓ LVIDs ↓ severity of myocardial damage ↓ cardiac fibrosis ↓ collagen fiber area ↓ LDH ↓ myocardial ultrastructural damage ↓ autophagosomes ↓ LC3 mRNA expression ↓ Beclin 1 mRNA expression ↓ Atg5 mRNA expression ↑ P62 mRNA expression ↓ LC3 II/I protein expression ratio ↓ Beclin 1 protein expression ↓ Atg5 protein expression ↑ P62 protein expression ↑ p-PI3K/PI3K protein expression ↑ p-Akt/Akt protein expression ↑ p-mTOR/mTOR protein expression	[9]
Hypoxia-treated H9c2 cells	Concurrent treatment 1 and 10 μM	↑ cell viability ↓ mitochondrial membrane depolarization ↓ ROS ↑ oxygen consumption rates in basal respiration ↑ ATP generation ↑ maximum respiration ↓ autophagic flux ↓ Beclin 1 protein expression ↓ Atg5 protein expression ↑ p62 protein expression	[9]

Abbreviation: +dP/dt: maximum rate of rise of left ventricular pressure over time; Ac-FOXO1: acetylated Forkhead box O1; ANP: atrial natriuretic peptide; Atg5: autophagy-related protein 5; ATP: adenosine triphosphate; BNP: brain natriuretic peptide; CK-MB: creatine kinase-MB; cTnT: cardiac troponin; EF: ejection fraction; LVEF: left ventricular ejection fraction; HW/TL: heart weight/tibia length ratio; FS: fractional shortening; mTOR: mammalian target of rapamycin; LC3: microtubule-associated protein 1A/1B-light chain 3; LDH: lactate dehydrogenase; LVIDd: left ventricular internal dimension at end-diastole; LVIDs: left ventricular internal dimension at end-systole; MDA: malondialdehyde; Nrf2: nuclear factor erythroid 2-related factor 2; ROS: reactive oxygen species; ↓: decreased; ↑: increased; ↔: no changes.

Emerging evidence indicates that columbianadin exerts potent immunomodulatory, anti-inflammatory, and bone-protective effects through the regulation of multiple rheumatoid arthritis-associated signaling pathways. Dendritic cells play a pivotal role in the initiation of RA by presenting autoantigens to T cells, thereby triggering synovial inflammation and cytokine release. Columbianadin suppresses dendritic cell maturation by downregulating the expression of cluster of differentiation (CD) molecules CD80 and CD86 and major histocompatibility complex class II, while preserving phagocytic function. In addition, it suppresses TNF-α-induced dendritic cell migration and reduces chemokine production, particularly MCP-1 and macrophage inflammatory protein-1α (MIP-1α), which are critical for immune cell recruitment to inflamed joints. These effects are associated with inhibition of the TLRs/MAPKs/NF-κB signaling pathways, as evidenced by reduced expression of TLR2, TLR7, TLR9, p-p38, p-JNK1/2,

and p-NF-κB [46].

Oral administration of *Angelicae pubescentis* radix water extract (decoction) in a male Sprague–Dawley rat model of adjuvant-induced arthritis reduced synovial cell proliferation, inflammatory cell infiltration, and pannus formation. Mass spectrometry analysis using ultra-high-performance liquid chromatography–quadrupole time-of-flight mass spectrometry (UHPLC-QTOF/MS) of blood plasma collected from the abdominal aorta detected columbianadin as a major absorbed compound in the bloodstream, suggesting that columbianadin may contribute to the observed anti-arthritic effects of the extract. In the same study, *in vitro* studies using human rheumatoid arthritis synovial fibroblasts (MH7A cells) demonstrated that columbianadin inhibited cell proliferation in a concentration- and time-dependent manner [47]. Furthermore, concurrent treatment with columbianadin (12.5, 25 and 50 μM) for 24–48 h suppressed TNF-α-induced proliferation and nitric oxide production in MH7A cells, while also inhibiting cell migration and invasion [48]. Mechanistically, columbianadin exerts its effects through coordinated regulation of apoptosis and autophagy pathways. It upregulates pro-apoptotic and autophagy-related proteins including Bax, p53, Beclin-1, while downregulating anti-apoptotic and autophagy-associated proteins such as Bcl-2 and p62. These effects are associated with inhibition of the vimentin-dependent Vav guanine nucleotide exchange factor 2/Ras-related C3 botulinum toxin substrate 1 (VAV2/Rac1) signaling axis. Columbianadin reduces vimentin expression, leading to suppression of downstream effectors, including Rac1, phosphorylated VAV2, and matrix metalloproteinases (MMP-2 and MMP-9), thereby limiting synoviocyte proliferation and invasive behavior. Importantly, genetic silencing of vimentin in TNF-α-stimulated MH7A cells recapitulated the effects of columbianadin, resulting in reduced proliferation and migration, alongside decreased expression of Rac1 and MMPs. These findings identify vimentin as a critical regulatory node in rheumatoid arthritis pathogenesis and suggest that it may represent an important molecular target of columbianadin through the VAV2/Rac-1 signaling pathway.

In a collagen-induced arthritis in male DBA/1 J mice, post-treatment with columbianadin (10, 20, and 40 mg/kg/day), administered orally from day 22 to day 66, significantly alleviated disease severity, as evidenced by reduced clinical arthritis score, foot and paw swelling, together with cartilage and bone erosions in the ankle joints. Histopathological analyses, including hematoxylin and eosin staining, toluidine blue staining, and micro-computed tomography, further confirmed that columbianadin ameliorated synovial inflammation, cartilage degradation, and bone destruction. Consistent with the *in vitro* findings, reduced expression of vimentin, Rac1, and the p-VAV2/VAV2 ratio was also observed *in vivo* (Table 6) [48]. Similarly, other collagen-induced arthritis studies have reported that columbianadin markedly suppresses pro-inflammatory cytokines, thereby inhibiting synovial hyperplasia and reducing paw swelling, inflammatory cell infiltration, and arthritis scores [30, 41]. Additional evidence indicates that columbianadin modulates key signaling pathways involved in RA progression, including the Janus kinase 1/signal transducer and activator of transcription 3 (JAK1/STAT3), NF-κB, Kelch-like ECH-associated protein 1 (Keap1)/Nrf2, and MAPK pathways. This regulation contributes to the restoration of oxidative balance through enhanced antioxidant enzyme activities, ultimately leading to reduced joint inflammation and structural damage [41].

Columbianadin has also been investigated in traumatic synovitis using a non-invasive anterior cruciate ligament tear (ACLT) model in mouse knees to mimic post-traumatic joint inflammation and early osteoarthritis. Treatment produced significant anti-inflammatory and joint-protective effects, including reductions in synovial hyperplasia, inflammatory cell infiltration, and the production of pro-inflammatory mediators such as iNOS, TNF-α and IL-1β [49]. Tripartite motif-containing protein 7 (TRIM7), which is highly expressed in the synovium of patients with rheumatoid arthritis, has been implicated in promoting cuproptosis, a copper-dependent form of cell death, in macrophages, thereby contributing to chronic joint inflammation and tissue damage [50]. TRIM7 interacts with zinc finger DHHC-type palmitoyltransferase 5 (ZDHHC5), which in turn associates with P2X7, facilitating subcellular translocation and copper efflux that may contribute to cuproptosis. Intra-articular administration of columbianadin significantly reduced copper accumulation in joint tissues, attenuated articular bone damage, and downregulated the expression of ferredoxin 1 (FDX1) and TRIM7, thereby reducing macrophage-associated cell death in synovial tissues. Additionally, columbianadin modulates synovial macrophage polarization, as evidenced by reduced M2 macrophage cell death and an increased M2/M1 macrophage ratio. M1 ($CD86^+$) synovial macrophages exhibit pro-inflammatory properties, whereas M2 ($CD206^+$) macrophages are generally associated with anti-inflammatory and tissue-reparative functions, suggesting that columbianadin promotes a shift toward a more anti-inflammatory macrophage profile

[49].

In addition to its anti-arthritic properties, columbianadin plays a role in regulating bone remodeling and exhibits significant osteoprotective effects. In a glucocorticoid-induced osteoporosis model in Sprague–Dawley rats, oral administration of columbianadin (5, 10, and 20 mg/kg) for 5 weeks significantly increased bone mineral content, bone mineral density, tissue mineral content, and tissue mineral density, accompanied by recovery of body and organ weights [14]. These effects were consistent with improvements in multiple bone turnover biomarkers, including reductions in tartrate-resistant acid phosphatase (TRAP), β-C-terminal telopeptide of type I collagen (β-CTX), bone Gla protein, acid phosphatase and alkaline phosphatase, alongside increases in osteocalcin, calcium, magnesium, and 25-hydroxyvitamin D levels. Columbianadin also restored hormonal homeostasis by increasing estradiol levels while reducing parathyroid hormone levels. Estrogen is essential for maintaining bone homeostasis by promoting osteoblast activity and inhibiting bone resorption, whereas parathyroid hormone increases serum calcium levels primarily by stimulating bone resorption [51, 52].

Beyond its effects on bone turnover and endocrine regulation, columbianadin may exert systemic protective effects through antioxidant, anti-inflammatory, and apoptosis-related mechanisms. Notably, columbianadin treatment in glucocorticoid-induced osteoporosis in rats reduced the expression of the anti-apoptotic genes Bcl-2 and X-linked inhibitor of apoptosis protein (XIAP) [14]. Interestingly, the expression of the pro-apoptotic caspase genes caspase-9, caspase-3, caspase-6, and caspase-7 was also reduced. These findings suggest that columbianadin may modulate apoptosis-related pathways in a complex manner, rather than causing a uniform increase or decrease in pro- or anti-apoptotic genes. The reduced expression of several caspase genes may indicate attenuation of apoptotic signaling at the transcriptional level; however, this cannot be confirmed without assessing caspase activation or protein expression. The anti-osteoporotic effects of columbianadin were further supported by improved bone mineralization, enhanced antioxidant defense, and reduced oxidative stress [14]. These effects may also involve the modulation of growth factors, including insulin-like growth factor (IGF) and transforming growth factor-beta (TGF-β). Mechanistically, columbianadin may promote osteogenesis by increasing the expression of bone morphogenetic proteins and upregulating runt-related transcription factor 2 (RUNX2), both of which are important for osteoblast differentiation. Concurrently, it may suppress osteoclastogenesis through modulation of the receptor activator of nuclear factor-κB ligand/osteoprotegerin (RANKL/OPG) axis, characterized by reduced RANKL signaling and enhanced OPG-mediated inhibition of osteoclast differentiation and activity [14].

Similarly, in an ovariectomized C57BL/6J mouse model, columbianadin exhibited anti-osteoporotic effects through inhibition of the S6K/filamin C/integrin β3 signaling pathway, as evidenced by decreased expression of acid phosphatase 5, RANKL, S6K, filamin C, and integrin β3 [15]. This downregulation improved bone microarchitecture and increased the maximum fracture force of the tibia, indicating enhanced bone strength in addition to reduced bone loss. Furthermore, an *in vitro* study using bone marrow-derived mononuclear cells isolated from mouse femurs and tibias demonstrated that columbianadin suppressed osteoclastogenesis induced by macrophage colony-stimulating factor (M-CSF) and RANKL. Specifically, it reduced TRAP activity, downregulated filamin C and integrin β3 expression, impaired F-actin ring formation, and decreased osteoclastic bone resorption activity. These findings indicate that columbianadin mitigates bone loss by coordinately regulating osteogenic and osteoclastic pathways. Its effects appear to involve modulation of the RANKL/OPG axis and inhibition of S6K/filamin C/integrin β3 signaling, alongside its antioxidant and anti-apoptotic properties, ultimately contributing to improvements in bone mass, microarchitecture, and mechanical strength.

Collectively, these findings demonstrate that columbianadin exerts dual protective effects on joint inflammation and bone metabolism. Through the simultaneous suppression of inflammatory signaling pathways and regulation of osteogenic and osteoclastic processes, columbianadin limits joint destruction, attenuates bone loss, and promotes skeletal homeostasis, highlighting its therapeutic potential for rheumatoid arthritis -associated bone disorders and osteoporosis.

Table 6. Bone-protective effects of columbianadin and columbianadin-containing extracts

Model	Dose	Findings	Reference
TNF-α-stimulated dendritic cells	Concurrent treatment 3, 6, 13, 25 and 50 μM, 36 h (purified columbianadin)	↓ maturation of TNF-α-induced dendritic cells ↓ CD11c ↓ CD40 ↓ CD80 ↓ CD86 ↓ major histocompatibility complex class II ↓ IL-6 mRNA expression ↓ MCP-1 ↓ MIP-1α ↓ TLR2 mRNA expression ↓ TLR7 mRNA expression ↓ TLR9 mRNA expression ↓ p38 protein expression ↓ JNK 1/2 protein expression ↓ NF-κB protein expression	[46]
Adjuvant-induced arthritis in male Sprague–Dawley rats	Post-treatment 3, 6 and 9 g/kg gavage, 12 days (columbianadin-containing *Angelicae pubescentis* radix extract)	↓ synovial cell proliferation ↓ inflammatory cell infiltration	[47]
MH7A cells	6.25–100 μg/ml (19.03-304.54 μM), 24-48 h (purified columbianadin)	↓ cell proliferation	[47]
Collagen-induced arthritis in female Wistar rats	Post-treatment 3, 6 and 9 g/kg gavage, 12 days (columbianadin-containing extract)	↓ degree of paw swelling ↓ inflammatory cells ↓ TNF-α ↓ IL-1β ↑ IL-10 ↓ p-ERK protein expression ↓ p-JNK protein expression ↓ p-p38 protein expression	[30]
Collagen-induced arthritis in male DBA/1 mice	Post-treatment, 20 mg/kg orally for 3 weeks (purified columbianadin)	↓ degree of paw swelling ↓ arthritis scores ↓ cartilage damage ↓ collagen fibers proliferation ↓ ankle injury ↓ inflammatory cell infiltration ↓ TNF-α ↓ TNF-α mRNA expression ↓ IL-1β ↓ IL-1β mRNA expression ↓ IL-6 ↓ IL-6 mRNA expression ↔ IL-10 ↑ IL-10 mRNA expression ↑ SOD ↑ GSH ↔ catalase ↓ STAT3 mRNA expression ↓ p-STAT3 protein expression ↔ JAK1 mRNA expression ↓ p-JAK1 protein expression ↓ p-NF-κB p65 protein expression ↓ p-IκBα protein expression ↓ p-50 protein expression ↓ Keap1 mRNA expression ↓ Keap1 protein expression ↑ Nrf2 mRNA expression ↑ Nrf2 protein expression ↑ HO-1 mRNA expression	[41]
Collagen-induced arthritis DBA/1 J mice	Post-treatment 10, 20 and 40 mg/kg/d, daily from day 22 to day 66 (purified columbianadin)	↓ degree of foot and paw swelling ↓ cartilage and bone erosions of ankle joint ↓ vimentin protein expression ↓ Rac-1 protein expression ↓ p-VAV2/VAV2 protein expression	[48]
TNF-α-induced proliferation and migration of MH7A cells	Concurrent treatment 12.5, 25 and 50 μM for 24–48 h (purified columbianadin)	↓ relative cell proliferation ↓ nitric oxide ↓ % of wound healing within 24h ↓ relative cell migration ↓ p62 protein expression ↑ beclin-1 protein expression ↑ bax protein expression ↓ bcl-2 protein expression ↑ p53 protein expression ↓ vimentin protein expression ↓ vimentin mRNA expression ↓ Rac-1 protein expression ↓ Rac-1 mRNA expression ↓ p-VAV2/VAV2 protein expression ↓ MMP-2 protein expression ↓ MMP-9 protein expression	[48]
Non-invasive anterior cruciate ligament tear	2, 4, 8 mg/joint, intra-articular	↓ M2 synovial macrophage death	[49]

Model	Dose	Findings	Reference
(ACLT) surgery in C57BL/6 mice	(purified columbianadin)	↑ M2/M1 synovial macrophage ratio ↓ iNOS ↓ TNF-α ↓ IL-1β ↓ TRIM7 protein expression ↓ FDX1 protein expression ↓ intracellular copper	
Glucocorticoid-induced osteoporosis in Sprague Dawley rats	Post-treatment 5, 10 and 20 mg/kg, orally for 5 weeks (purified columbianadin)	↑ body weight ↑ organs weight ↑ bone mineral content ↑ bone mineral density ↑ tissue mineral content ↑ tissue mineral density ↓ TRAP ↑ osteocalcin ↓ β-CTX ↓ bone Gla protein ↓ acid phosphatase ↓ ALP ↑ phosphorus ↑ calcium ↑ magnesium ↑ 25 (OH) vitamin D levels ↑ estradiol ↓ parathyroid hormone ↑ GPx ↓ TBARS ↑ catalase ↑ SOD levels ↑ GSH levels ↓ TNF-α levels ↓ IL-1β levels ↓ IL-6 levels ↑ IGF levels ↑ TGF-β levels ↓ RANKL levels ↓ OPN ↑ OPG ↑ OPG/RANKL ↑ ALP mRNA expression ↑ OCN mRNA expression ↑ OPN mRNA expression ↑ RunX2 mRNA expression ↑ BMP-2 mRNA expression ↑ BMP-4 mRNA expression ↑ BMP-6 mRNA expression ↑ BMP-7 mRNA expression ↑ BMP-9 mRNA expression ↓ Bcl2 mRNA expression ↓ BclxL mRNA expression ↑ IAP1 mRNA expression ↓ IAP2 mRNA expression ↓ XIAP mRNA expression ↓ caspase-6 mRNA expression ↓ caspase-3 mRNA expression ↓ caspase-7 mRNA expression ↓ caspase-9 mRNA expression	[14]
Ovariectomized female C57BL/6 J mice	Post-treatment 12.5, 25, and 50 mg/kg, i.g. for 10 weeks (purified columbianadin)	↔ body weight and organs ↑ whole-body bone mineral densities ↑ whole-body bone mineral masses ↑ lumbar whole-body bone mineral densities ↑ tibia whole-body bone mineral densities ↑ femur whole-body bone mineral densities ↑ maximum fracture force of the tibia ↑ number of bone trabeculae in the femoral epiphysis ↓ acid phosphatase 5 ↓ RANKL ↓ S6 K protein expression ↓ filament C protein expression ↓ ITGβ3 protein expression	[15]
MCSF and RANKL-induced osteoclastogenesis in BMMs	0.1, 1, and 10 μM (purified columbianadin)	↓ osteoclast development ↔ osteoclast precursor cell activity ↓ TRAP activity ↓ TRAP protein expression ↓ S6K protein expression ↓ c-Fos protein expression ↓ NFATc1 protein expression ↓ filament C protein expression ↓ ITGβ3 protein expression ↓ development F-actin rings ↓ osteoclast bone resorption activity	[15]

Abbreviation: β-CTX: β-C-terminal telopeptide of type I collagen; ALP: alkaline phosphatase; BcLxL: B-cell lymphoma-extra-large; BMMs: bone marrow–derived

mononuclear cells; BMP: bone morphogenetic proteins; CD: cluster of differentiation; ERK: extracellular signal-regulated kinase; FDX1: ferredoxin 1; GSH: glutathione; GPx: glutathione peroxidase; i.g.: intragastric; HO-1: heme oxygenase-1; IAP: inhibitor of apoptosis protein; IGF: Insulin-like growth factor; IAP: inhibitor of apoptosis protein; IL: interleukin; iNOS: inducible nitric oxide synthase; ITGβ3: integrin β3; JAK1: Janus kinase 1/signal transducer; JNK 1/2: c-Jun N-terminal kinase 1/2; Keap1: Kelch-like ECH-associated protein 1; MCSF: macrophage-stimulating factor; MCP-1: monocyte chemoattractant protein-1; MIP-1α: macrophage inflammatory protein-1α; MH7A: human rheumatoid arthritis synovial cell line; MMP: metalloproteinase; NFATc1: nuclear factor of activated T-cells 1; NF-κB: nuclear factor κ-light-chain-enhancer of activated B cells; OCN: osteocalcin; OPG: osteoprotegerin; OPN: osteopontin; Rac-1: Ras-related C3 botulinum toxin substrate 1; RANKL: receptor activator of NF-κB ligand; RunX2: runt-related transcription factor 2; S6K: Ribosomal Protein S6 Kinase; SOD: superoxide dismutase; STAT3: signal transducer and activator of transcription 3; TBARS: thiobarbituric acid reactive substances; TGF-β: transforming growth factor; TNF-α: tumor necrosis factor-α; TRAP: tartrate-resistant acid phosphatase; TLRs: Toll-like receptors; TRIM7: tripartite motif-containing protein 7; VAV2: Vav guanine nucleotide exchange factor 2; XIAP: X-linked inhibitor of apoptosis protein; ↓: decreased; ↑: increased; ↔: no changes.

5.7 Antiplatelet and antithrombotic activities

Platelet aggregation is a critical step in thrombus formation and plays a central role in the pathogenesis of thromboembolic disorders, including myocardial infarction, stroke, and deep vein thrombosis. Inhibition of platelet aggregation represents an important therapeutic strategy for reducing the risk of pathological clot formation [53]. Columbianadin has demonstrated promising antiplatelet activity [10]. Evaluation of its inhibitory effects on human platelet aggregation induced by various agonists revealed that columbianadin (40–80 μM) selectively inhibited collagen-induced platelet aggregation with an approximate half-maximal inhibitory concentration (IC_{50}) of 60 μM, while showing no significant effects on aggregation triggered by other agonists, including thrombin, U46619, and arachidonic acid. Platelet activation is associated with intracellular calcium mobilization and the release of platelet granule contents, including P-selectin and ADP/ATP [54]. Columbianadin inhibited intracellular calcium mobilization and the release of these platelet activation mediators, thereby attenuating platelet activation. Furthermore, columbianadin (60-160 μM) did not significantly affect platelet lactate dehydrogenase release, indicating an absence of cytotoxicity and suggesting that its antiplatelet activity is not associated with membrane damage or platelet cytolysis (Table 7).

The antiplatelet activity of columbianadin is mainly associated with inhibition of the phospholipase Cγ2–protein kinase C (PLCγ2–PKC) signaling pathway, which is essential for collagen-induced platelet activation [55]. Columbianadin suppresses phosphorylation of PLCγ2 and the PKC substrate protein p47. However, this effect is unlikely to result from direct PKC inhibition, as phorbol 12,13-dibutyrate (PDBu)-induced PKC activation remains unaffected. Instead, columbianadin appears to act at an upstream regulatory level by suppressing Akt and MAPK signaling pathways, as evidenced by reduced phosphorylation of PLCγ2, p47, Akt, ERK1/2, and JNK1/2. Columbianadin also has no effect on vasodilator-stimulated phosphoprotein (VASP) phosphorylation, indicating that its antiplatelet effects are independent of the cyclic nucleotide–VASP pathway.

The antithrombotic efficacy of columbianadin was demonstrated in a mesenteric microvascular injury mouse model, in which it significantly prolonged time to vessel occlusion and inhibited thrombus formation, demonstrating functional protection against vascular thrombosis. As platelet aggregation and thrombus stabilization are mediated by fibrinogen binding to integrin αIIbβ3, the effect of columbianadin on this pathway was also examined. Consistent with these findings, columbianadin did not interfere with integrin αIIbβ3-mediated outside-in signaling, as fibrinogen-induced phosphorylation of integrin β3, Src, and focal adhesion kinase (FAK) remained unchanged. Additionally, columbianadin dose-dependently reduced mortality in an ADP-induced acute pulmonary thromboembolism mouse model, demonstrating efficacy against severe systemic thrombotic events [10]. These findings suggest that columbianadin may exert antithrombotic effects by acting on early intracellular signaling pathways upstream of integrin αIIbβ3 activation, without significantly affecting integrin-mediated outside-in signaling.

In another study, platelet adhesion and plug formation were evaluated using a high-shear-flow thrombosis model based on microfluidic flow chambers, in which human whole blood was perfused over a collagen ± ADP-coated membrane to mimic arterial thrombosis under high-shear-stress conditions [11]. Pretreatment with 90 μM columbianadin for 2 min significantly prolonged the closure time of the aperture in whole blood. However, post-treatment with columbianadin (10–20 mg/kg, i.p.), for 30 min in a tail-transection bleeding-time mouse model did not significantly prolong bleeding time. In contrast, aspirin-treated mice (positive control) showed a marked prolongation of bleeding time under the same conditions. These findings suggest that, unlike aspirin, columbianadin may exert antithrombotic effects without substantially increasing the risk of bleeding [11]. Columbianadin also inhibited collagen-induced human platelet aggregation and reduced ATP release. In addition, it attenuated hydroxyl radical formation, resulting in reduced oxidative stress, which is known to contribute to platelet activation. This antioxidant effect may further support its antiplatelet activity. Mechanistically, these effects were associated with

inhibition of the NF-κB and MAPK signaling pathways, as evidenced by reduced phosphorylation of nuclear factor of κB inhibitor α (IκBα), p65, ERK1/2, and JNK1/2, as well as suppression of IκBα degradation. The involvement of these pathways was further substantiated using specific NF-κB and MAPK inhibitors, which elicited effects on platelet activation similar to those of columbianadin, supporting their role in mediating its antiplatelet activity [11].

Taken together, these findings suggest that columbianadin exerts antiplatelet and antithrombotic effects through selective inhibition of collagen-mediated platelet activation, primarily involving modulation of the PLCγ2–PKC, MAPK, and NF-κB signaling pathways, while preserving integrin αIIbβ3-dependent hemostatic function and potentially reducing the risk of bleeding.

5.8 Anticancer property

Columbianadin exhibited cytotoxic effects in HCT-116 human colorectal cancer cells by inducing programmed cell death through both apoptotic and necroptotic pathways, highlighting its potential as a natural product-derived candidate for colorectal cancer therapy [13]. Treatment with columbianadin (0–100 μM) resulted in dose- and time-dependent inhibition of cell growth, with IC_{50} values of 47.2 and 32.4 μM after 48 and 72 h of incubation, respectively. Pronounced morphological changes, including cell rounding and cell death, were observed in cells treated with 25 and 50 μM columbianadin. Cell cycle analysis revealed a significant increase in the sub-G_1 population, indicative of apoptotic cell death, which was consistent with annexin V staining showing an increased proportion of apoptotic cells. These effects were associated with the modulation of key apoptosis-related proteins, including cleaved caspase-9, cleaved caspase-3, Bax, p53, and Bcl-2.

Table 7. Antiplatelet and antithrombotic effects of columbianadin

Model	Dose	Findings	Reference
Collagen-induced human platelet aggregation	40–160 μM	↓ % aggregation, $IC_{50} \approx 60$ μM ↓ LDH activity (%) ↓ surface P-selectin expression ↓ ATP release reaction ↓ Calcium mobilization ↓ p-PLCγ2/PLCγ2 protein expression ↓ p-p47/p47 protein expression ↔ PDBu-induced platelet aggregation ↓ p-Akt/Akt protein expression ↓ p-ERK 1/2/ERK 1/2 protein expression ↓ p-JNK 1/2/JNK 1/2 protein expression ↔ p-p38/p38 protein expression ↔ p-VASP/VASP protein expression ↓ PAC-1 binding ↔ fibrin clot retraction ↔ FITC-triflavin binding	[10]
Thrombin-induced human platelet aggregation	40–160 μM	↔ % aggregation	[10]
U46619-induced human platelet aggregation	40–160 μM	↔ % aggregation	[10]
Arachidonic acid-induced human platelet aggregation	40–160 μM	↔ % aggregation ↔ ATP release reaction ↔ p-Akt/Akt protein expression	[10]
Platelets exposed to a fibrinogen-coated surface	60 and 80 μM	↔ p-integrin β_3 protein expression ↔ p-Src protein expression ↔ p-FAK protein expression	[10]
Sodium fluorescein-induced vascular thrombus formation in mouse mesenteric microvessels	5 and 10 mg/kg, i.v.	↑ occlusion time of thrombotic platelet plug formation	[10]
ADP-induced acute pulmonary thromboembolism in mice	5 and 10 mg/kg, i.p., once during experiment	↓ number of deaths and mortality (%)	[10]
High-shear-flow-induced platelet plug formation in human whole blood using a collagen/ADP-coated membrane	Pretreatment 90 μM, 2 min	↑ closure time of aperture	[11]
Tail-transection bleeding-time assay in mice	Post-treatment 10–20 mg/kg, i.p., 30 min	↔ bleeding time	[11]
Collagen-induced human platelet aggregation	Pre-treatment, 90 μM, 3 min	↓ % aggregation ↓ ATP release ↓ p-IκBα protein expression ↓ p-p65 protein expression ↑ IκBα protein expression ↓ p-ERK 1/2 protein expression ↓ p-JNK 1/2 protein expression ↓ hydroxyl radical	[11]

Abbreviation: ATP: adenosine triphosphate; FAK: focal adhesion kinase; FITC, fluorescein isothiocyanate; IC_{50}: half-maximal inhibitory concentration; LDH: lactate dehydrogenase; PAC-1, anti-human CD41/CD61 activation-dependent monoclonal antibody; PDBu: phorbol 12,13-dibutyrate; p-AKT: phosphorylated protein kinase B; p-ERK: phosphorylated extracellular signal-regulated kinase; p-IκBα: phosphorylated nuclear factor of κB inhibitor α; p-JNK: phosphorylated c-Jun N-terminal kinase; p-PLCγ2: phosphorylated phospholipase Cγ2; VASP: vasodilator-stimulated phosphoprotein; ↓: decreased; ↑: increased; ↔: no changes.

The expression levels of Bcl-2-interacting mediator of cell death (Bim) and BH3-interacting domain death agonist (Bid) were also reduced in association with the observed apoptotic response. Bim and Bid are BH3-only proteins involved in mitochondrial apoptotic signaling, although Bid can also link the extrinsic and intrinsic apoptotic pathways following caspase-8-mediated cleavage to form truncated Bid (tBid). Despite the increased levels of cleaved caspase-9 and caspase-3, the reduction in Bim and Bid suggests that these BH3-only proteins may not be the primary mediators of the observed apoptotic response. The activation of caspase-9 and caspase-3 nevertheless supports the involvement of the intrinsic apoptotic pathway [13]. The concurrent suppression of caspase-8 activation and Bid expression, together with increased receptor-interacting protein kinase-3 (RIPK-3) expression, is consistent with the possible involvement of RIPK3-associated necroptotic signaling. Thus, necroptosis may contribute to cell death alongside apoptotic signaling, rather than necessarily replacing it [56]. Furthermore, the downregulation of Bim suggests that Bim may not be the sole mediator of the observed apoptotic response, particularly in view of the concurrent modulation of p53 and Bax. Nevertheless, these findings do not establish a definitive shift from intrinsic apoptosis toward necroptosis, nor do they demonstrate that apoptosis is predominantly mediated through ROS-induced mitochondrial dysfunction or p53/Bax activation. The observed cleavage of poly(ADP-ribose) polymerase (PARP) provides additional evidence of programmed cell death pathway activations [57].

Furthermore, columbianadin increased intracellular ROS accumulation and disrupted antioxidant enzyme homeostasis, potentially contributing to apoptosis- and necroptosis-mediated cytotoxicity. Specifically, it downregulated catalase and SOD-1 while increasing SOD-2 and GPx1 expression, with no significant effects on thioredoxin or peroxiredoxin I/II. The differential regulation of SOD isoforms may reflect distinct cellular responses to oxidative stress, as SOD1 is primarily localized in the cytosol and contributes to ROS detoxification, whereas SOD2 is localized in the mitochondria and plays a critical role in controlling mitochondrial oxidative stress [58, 59]. The increase in SOD2 may therefore represent a compensatory mitochondrial antioxidant response, whereas reduced SOD1 expression may be associated with increased ROS accumulation during columbianadin-induced cancer cell death. These findings suggest that columbianadin-mediated regulation of antioxidant enzymes involves modulation of SOD, GPx1, and catalase, with no significant effects on thioredoxin or peroxiredoxin I/II in human colorectal cancer cells (Table 8). Collectively, these findings suggest that columbianadin suppresses HCT 116 colorectal cancer cell viability through the induction of apoptosis and necroptosis, potentially involving modulation of key signaling proteins and oxidative stress-related mechanisms [13]. However, these findings are primarily based on *in vitro* data from a single cell line and may not fully recapitulate the complexity of tumors *in vivo*.

In addition, columbianadin demonstrated anti-glioblastoma activity in rat C6 glioma cells and human DBTRG glioblastoma cells, as well as in an orthotopic glioblastoma mouse model established by intracranial implantation of GL261 cells into C57BL/6J mice [60]. In both C6 and DBTRG cell lines, columbianadin inhibited cell viability and proliferation by inducing cell cycle arrest at the G_0/G_1 phase. This effect was accompanied by the downregulation of cyclin D1, a key regulator of G_1/S phase transition, thereby contributing to the suppression of glioblastoma cell proliferation [61]. Furthermore, columbianadin induced apoptosis and inhibited the migration and invasion of glioblastoma cells, accompanied by reduced expression of N-cadherin, vimentin and MMP-2 and 9. Findings from the orthotopic glioblastoma model further supported these *in vivo* observations, demonstrating a reduction in tumor volume following columbianadin treatment [60]. These antitumor effects were associated, at least in part, with modulation of the PI3K/Akt signaling pathway, as evidenced by the downregulation of proteins involved in this pathway.

Collectively, these findings suggest that columbianadin suppresses glioblastoma progression by inhibiting cellular migration and invasion, potentially through modulation of the PI3K/Akt signaling pathway. Nevertheless, further validation in multiple experimental models is warranted to establish its therapeutic potential and to better characterize its pharmacokinetic properties and safety profile.

5.9 Antinociceptive effects

Neuropathic pain is a chronic pain condition that arises from injury or dysfunction of the somatosensory nervous system at either the peripheral or central level. Unlike nociceptive pain, which results from direct tissue damage, neuropathic pain is characterized by maladaptive neuronal signaling that produces symptoms such as allodynia, hyperalgesia, and spontaneous pain. Current pharmacological treatments, including antidepressants, anticonvulsants, and opioids, often fail to achieve satisfactory pain relief and are limited by adverse effects [62]. This has stimulated interest in natural

bioactive compounds with neuroprotective and analgesic properties, with columbianadin emerging as a promising candidate due to its anti-inflammatory, antioxidant, and analgesic activities [12]. In a mouse model of oxaliplatin-induced neuropathic pain, columbianadin (1–10 mg/kg, intraperitoneal) dose-dependently attenuated mechanical allodynia, defined as pain elicited by normally innocuous stimuli, and cold hyperalgesia, characterized by an exaggerated pain response to mildly noxious cold stimuli [12, 63]. Peripheral sensitization is a key feature of neuropathic pain, in which ion channels expressed in nociceptive dorsal root ganglion neurons play critical roles in transmitting pain signals from the periphery to the spinal cord [64]. Mechanistically, columbianadin inhibited voltage-gated calcium currents (*Ica*) in small dorsal root ganglion neurons, with preferential inhibition of T- and L-type calcium channels, which may contribute to its antinociceptive effects in this model [12]. These findings suggest that the combined inhibition of T- and L-type calcium channels by columbianadin may contribute to its antinociceptive activity and therapeutic potential in neuropathic pain. Nevertheless, further studies are warranted to clarify its precise molecular mechanisms and calcium channel subtype selectivity.

Table 8. Anticancer effects of columbianadin

Model	Dose	Findings	Reference
HCT116	12.5–50 μM	↓ growth of cells ↑ sub-G_1 phase ↑ cleaved caspase-9 protein expression ↑ cleaved caspase-3 protein expression ↑ Bax protein expression ↑ p53 protein expression ↓ Bcl-2 protein expression ↓ Bim protein expression ↓ Bid protein expression ↑ apoptotic cells ↑ necroptotic cells ↑ RIPK-3 protein expression ↓ cleaved caspase-8 ↑ cleaved PARP protein expression ↑ reactive oxygen species ↓ catalase protein expression ↓ SOD-1 protein expression ↑ SOD-2 protein expression ↑ GPx-1 protein expression ↔ thioredoxin ↔ peroxiredoxin-1 ↔ peroxiredoxin I/II	[13]
C6	30 μM, 24h	↓ cell viability and proliferation ↓ cell mitotic marker protein PH3 ↑ G_0-G_1 phase ↓ cyclin D1 protein expression ↓ Bcl-2/Bax protein expression ↑ cleaved caspase-3 positive cells ↓ cell migration and invasion ↓ N-cadherin protein expression ↓ vimentin protein expression ↓ MMP-2 mRNA expression ↓ MMP-9 mRNA expression ↓ p-PI3K P85/PI3K P85 protein expression ↓ p-AKT/AKT protein expression ↓ p-AKT fluorescence intensity	[60]
DBTRG	35 μM, 24h	↓ cell viability and proliferation ↓ cell mitotic marker protein PH3 ↑ G_0-G_1 phase ↓ cyclin D1 protein expression ↓ Bcl-2/Bax protein expression ↑ cleaved caspase-3 positive cells ↓ cell migration and invasion ↓ N-cadherin protein expression ↓ vimentin protein expression ↓ MMP-2 mRNA expression ↓ MMP-9 mRNA expression ↓ p-PI3K P85/PI3K P85 protein expression ↓ p-AKT/AKT protein expression ↓ p-AKT fluorescence intensity	[60]
Orthotopic glioblastoma in C57BL/6J mice	Post-treatment 20 mg/kg for 12 days, i.p.	↓ volume of tumors ↓ p-PI3K P85/PI3K P85 protein expression ↓ p-AKT/AKT protein expression	[60]

Abbreviation: Akt: protein kinase-B; Bax: Bcl-2-associated X protein; Bcl-2: B cell lymphoma 2; Bid: BH3 interacting death domain; Bim: Bcl-2-interacting mediator of cell death; C6: rat glioma cell line; DBTRG: human glioblastoma cell line; GPx: glutathione peroxidase; HCT116: human colorectal cancer cells; i.p.: intraperitoneal; MMP: matrix metalloproteinase; PARP: Poly (ADP-ribose) polymerase; PH3: phosphorylated histone H3; PI3K: phosphatidylinositol 3-kinase; RIP-3: receptor interaction protein kinase-3; SOD: superoxide dismutase; ↓: decreased; ↑: increased; ↔: no changes.

5.10 Anti-viral activity

Columbianadin has been identified as a potential multi-target direct-acting antiviral candidate based on its predicted interactions with the highly conserved nucleotide-binding pockets of several essential severe acute respiratory syndrome coronavirus 2 (SARS-CoV-2) proteins, including nonstructural protein 12 (NSP12), NSP13, NSP14, NSP15, and NSP16. These predicted interactions may interfere with the sites involved in viral RNA replication, helicase-mediated unwinding, and mRNA capping, potentially disrupting multiple stages of the viral life cycle. This multi-target activity was associated with a median effective concentration (EC_{50}) of 22.52 μM, suggesting antiviral activity against SARS-CoV-2 [16]. However, the extent to which these predicted interactions contribute to the observed antiviral effects remains to be experimentally established. Future studies should focus on validating the antiviral activity of columbianadin in cellular and *in vivo* infection models while addressing key translational challenges, including pharmacokinetics, bioavailability, safety, and efficacy against emerging SARS-CoV-2 variants. Further structural investigations may also provide insights into the optimization of columbianadin as a multi-target antiviral candidate.

6. Context-Dependent Pharmacological Effects

Although the pharmacological activities of columbianadin generally demonstrate consistent beneficial effects across experimental models, several findings reveal apparent discrepancies in pathway regulation and pharmacological responses. These differences are particularly evident in autophagy, MAPK signaling, antioxidant enzyme regulation, osteogenic marker expression, bioavailability, and potency. Such divergent observations should not necessarily be interpreted as contradictory evidence; rather, they may reflect differences in dose, exposure duration, experimental model, cell type, route of administration, disease state, and the chemical form of columbianadin. Differences in the biological level and timing of measurement may also contribute to apparent discrepancies between transcriptional and biochemical outcomes. Representative mechanistic discrepancies across experimental variables are summarized in Table 9.

In mice with left anterior descending coronary artery ligation-induced acute myocardial infarction and in hypoxia-treated H9c2 cardiomyocytes, columbianadin inhibited excessive autophagic activity through modulation of the PI3K/Akt/mTOR pathway, accompanied by reductions in LC3-II, Beclin-1, and Atg5 levels [9]. Conversely, in rheumatoid arthritis synoviocytes (MH7A cells), columbianadin promoted autophagy, as indicated by increased Beclin-1 and decreased p62 expression, thereby facilitating synoviocyte clearance and limiting hyperproliferation [48]. This apparent dual functionality suggests that columbianadin does not act as a simple agonist or antagonist of autophagy. Rather, its effects appear to depend on the underlying pathological stimulus, cell type, and cellular stress state. In cardiomyocytes subjected to cytotoxic or hypoxic stress, attenuation of excessive autophagy may contribute to cellular protection, whereas induction of autophagy in hyperproliferative synoviocytes may promote the elimination of pathogenic cells [48]. Thus, the biological consequences of autophagy modulation may depend not only on the direction of pathway regulation but also on whether autophagic activity is excessive, impaired, or therapeutically beneficial within a particular disease context.

A similar context-dependent pattern is observed in MAPK signaling, particularly with respect to p38 phosphorylation. Jayakumar et al. [4] reported that p38 MAPK phosphorylation remained unaffected in LPS-stimulated RAW 264.7 macrophages following a brief 20-min pretreatment with columbianadin (20–40 μM), whereas Ma et al. [6] observed significant suppression of p38 MAPK activation in a D-galactose-induced aging mouse model following chronic oral administration of columbianadin (200–800 mg/kg) for 8 weeks. These apparently divergent findings may be attributable to differences in dose, experimental model, cell type, route of administration, and treatment duration. The *in vitro* study examined an acute response in a macrophage cell line, whereas the *in vivo* study evaluated the effects of prolonged systemic exposure in an aging model. Differences in absorption, metabolism, tissue distribution, and upstream kinase regulation may therefore contribute to the distinct p38 responses. However, these explanations remain speculative because the studies did not directly compare these variables. Further mechanistic investigations are therefore required to determine whether p38 MAPK regulation by columbianadin depends on exposure conditions, experimental model, or disease context.

Table 9. Mechanistic discrepancies across experimental variables

Target	Observed Discrepancy	Representative findings	Potential contributing variables
p38 MAPK	Downregulated vs. unchanged	Suppressed in D-galactose-induced liver injury in mice [6]; unchanged in LPS-stimulated RAW 264.7 macrophages [4]	Dose, duration, route, cell/tissue context, model
Autophagic flux	Inhibited vs. promoted	Inhibited in acute myocardial injury mice [9]; promoted in MH7A cells [48]	Cell type, pathological stimulus, disease state, duration
SOD isoforms	Differential regulation	Increased total SOD activity [6]; decreased SOD1 but increased SOD2 [13]	Subcellular localization, cell type, disease state, oxidative stress
Osteogenic markers	Differential regulation	Decreased circulating levels of (ALP and OPN), but increased ALP and OPN mRNA expression in bone tissue [14]	Biological compartments, compensatory transcriptional responses, distinct kinetics of transcription, protein turnover
Pharmacokinetics	Different exposure profiles	Faster absorption with plant extract; higher bioavailability with pure columbianadin [23]	Chemical form, matrix effects, absorption, metabolism

Abbreviation: ALP: alkaline phosphatase; LPS: lipopolysaccharide; MAPK: mitogen-activated protein kinase; MH7A: human rheumatoid arthritis synovial cell line; OPN: osteopontin; SOD: superoxide dismutase

Context dependence is also evident in the regulation of antioxidant enzymes. Although columbianadin has been reported to increase total SOD activity in an aging model, its effects on individual SOD isoforms appear more complex, with decreased cytosolic SOD1 but increased mitochondrial SOD2 reported in HCT-116 cells [6, 13]. This apparent discrepancy may reflect differences in subcellular localization, cellular metabolic state, and the nature of the oxidative stress experienced by the cells. Therefore, assessment of total antioxidant enzyme activity alone may not fully capture the molecular effects of columbianadin on endogenous antioxidant defenses.

A related transcriptional–biochemical divergence was observed for the osteogenic markers alkaline phosphatase (ALP) and osteopontin (OPN) in glucocorticoid-induced osteoporosis [14]. Although their circulating biochemical levels were decreased, the corresponding mRNA expression levels in bone tissue were increased. This apparent discrepancy may reflect differences in the biological compartments measured, compensatory transcriptional responses, and the distinct kinetics of mRNA and protein turnover. Circulating biochemical levels are influenced by protein production, release, distribution, clearance, and degradation, whereas tissue mRNA expression reflects gene transcription within the sampled bone tissue. Prolonged glucocorticoid exposure may impair osteoblast function, protein synthesis or secretion, and extracellular matrix turnover, potentially contributing to reduced biochemical levels despite increased mRNA expression. The elevated ALP and OPN mRNA levels may therefore represent an adaptive response to impaired osteoblast function, although this mechanism has not been directly established [65, 66]. Furthermore, mRNA expression does not necessarily correlate with protein abundance or enzymatic activity, and differences in measurement timing may capture distinct stages of the biological response. Therefore, these findings should be interpreted cautiously, and further studies measuring gene expression, protein abundance, and functional activity concurrently are needed to clarify the underlying mechanisms.

Differences in pharmacological responses may also arise from the chemical and pharmacokinetic context in which columbianadin is administered. Extract-based preparations may exhibit different exposure profiles and potency compared with purified columbianadin because of matrix effects, synergistic interactions with other constituents, and differences in absorption and metabolism [23]. Thus, findings obtained using crude or enriched extracts should be interpreted cautiously when extrapolating the pharmacokinetic activity or pharmacokinetic behavior of purified columbianadin.

Collectively, these observations indicate that the pharmacological effects of columbianadin cannot always be interpreted as uniform pathway activation or inhibition. Instead, its biological activity appears to be shaped by the interplay of dose, exposure duration, route of administration, cell type, disease state, pathological stimulus, subcellular localization, and chemical form. Recognizing these sources of variability is important for reconciling apparently conflicting findings and determining which experimental observations are most relevant to the potential clinical application of columbianadin.

7. Toxicity Assessment of Columbianadin

Acute toxicity evaluation demonstrated that oral administration of columbianadin at doses of up to 2000 mg/kg did not cause mortality or observable behavioral abnormalities in mice during the 7-day observation period. Compared with the control group, no significant changes were observed in the body weight of either male or female mice in the treatment groups. In addition, organ indices, including those of the liver, kidney, heart, and spleen, were comparable

between the treated and control groups. Serum biochemical analysis further revealed that AST and ALT levels remained unchanged, indicating that columbianadin at a dose of 2000 mg/kg did not induce hepatotoxicity in mice [41]. These findings suggest that oral administration of columbianadin at doses of up to 2000 mg/kg is relatively safe and non-toxic under the conditions of this acute toxicity study. Similarly, Xiao et al. (2026) demonstrated the biosafety of columbianadin in a spinal cord injury model using female Sprague Dawley rats [40]. Histopathological examination revealed no significant abnormalities in major organs, including the heart, liver, spleen, lung, and kidney, suggesting the absence of overt toxicity. Furthermore, biochemical markers of liver and kidney function, including AST, ALT, blood urea nitrogen, and creatinine, remained within normal physiological ranges, indicating that columbianadin did not induce appreciable systemic toxicity in treated rats.

8. Conclusions and Future Directions

Columbianadin exhibits a broad spectrum of pharmacological activities, with its mechanisms of action investigated across various *in vitro* and *in vivo* preclinical models. Available evidence suggests that it modulates multiple interconnected signaling pathways involved in inflammation, oxidative stress, and immune regulation, thereby contributing to its hepatoprotective, gastroprotective, neuroprotective, cardioprotective, antiplatelet, anticancer, antinociceptive, and antiviral effects (Figure 3). This multi-target profile highlights its potential as a pleiotropic agent for the management of complex, multifactorial diseases. However, these pharmacological effects have been demonstrated primarily in experimental models, and their relevance to human disease remains to be established. Furthermore, the substantial difference between the concentrations used in some *in vitro* studies and the systemic exposure reported in rats raises important questions regarding the translational relevance of the reported pharmacological activities. Although these findings provide evidence of biological activity and potential molecular targets, effects observed at high micromolar concentrations should not automatically be interpreted as therapeutically relevant mechanisms. Further validation at lower, exposure-relevant concentrations, supported by target-specific experiments and integrated pharmacokinetic–pharmacodynamic analyses, is needed to distinguish physiologically relevant pharmacological activity from concentration-dependent or nonspecific effects. Despite these promising findings, the current evidence is insufficient to establish the clinical efficacy or safety of columbianadin and support its clinical translation at this stage. Important gaps persist in our understanding of its pharmacokinetics, long-term safety, and clinical efficacy in humans, limiting a comprehensive evaluation of its toxicological and therapeutic profiles. Further studies, including systematic toxicity evaluation, pharmacokinetic and bioavailability studies, formulation optimization, and well-designed clinical trials, are required to determine its potential for clinical application.

MARKER / MODEL	Inflammatory cytokines	Inflammatory mediators & enzymes	Oxidative stress	Antioxidant enzymes and regulator	Apoptosis & cell death markers	Upstream signaling / pathology cascades	Specific functional / phenotypic markers
GIT	TNF-α, IL-1β, IL-6, IL-8, IL-17, IL-18	COX-2, PGE_2, IFN-γ, MCP-1, NO	ROS, H_2O_2, LDH, MPO	SOD, GPx catalase, Nrf-2, HO-1	Bax, caspase	MAPK, PAI-1, NOD1, NF-κB, TLR4, TGF-β	Iron, calcium, gastric secretion
	IL-10				Bcl-2		Sulfhydryl, ZO-1, Ocln
Neuro	TNF-α, IL-1β,	COX-2, iNOS, M1 phenotype			Apoptotic cells	PTEN, PI3K/Akt	Neural regeneration
					Bcl-xL		
Liver						Fibrosis	AST, ALT, Suzuki score
Cardiac			ROS, MDA, LDH	Catalase, Nrf-2, HO-1	Caspase, Bax	Ac-FOXO1, fibrosis	LDH, cTnT, CK-MB, ANP, BNP
					Bcl-2	Sirt1	
Bone	TNF-α, IL-1β, IL-6	MCP-1, iNOS		Nrf-2, HO-1, SOD, GSH, catalase	Caspase, Bcl-xL	p-VAV2 JAK1/STAT3, NF-κB, MAPKs, TLR	RANKL, β-CTX, OPN
	IL-10						BMP, RunX, IAP1
Vascular			LDH, ROS			MAPK, p-IκBα, NF-κB, p-PLCγ2, PI3K/Akt	
Cellular				SOD, catalase	Bcl-2, Bim, Bid	PI3K, Akt	Proliferation, Cell migration
					Bax, p53	RIPK-3	Sub-G1
Peripheral nerve							*Ica*

Decreased Increased Not evaluated

Figure 3. System pharmacology heatmap of columbianadin across experimental disease models. Abbreviation: β-CTX: β-C-terminal telopeptide of type I collagen; Ac-FOXO1: acetylated Forkhead box O1; AKT: protein kinase B; ALT: alanine aminotransferase; ANP: atrial natriuretic peptide; AST: aspartate aminotransferase; Bax: Bcl-2-associated X protein; Bcl-2: B-cell lymphoma 2; Bcl-xL: B-cell lymphoma-extra large; Bid: BH3 interacting death domain; Bim: Bcl-2-interacting mediator of cell death; BNP: brain natriuretic

peptide; CK-MB: creatine kinase-MB; COX-2: cyclooxygenase; cTnT: cardiac troponin T; GIT: gastrointestinal tract; GPx: glutathione peroxidase; GSH: glutathione; H_2O_2: hydrogen peroxide; HO-1: heme oxygenase-1; IAP1: inhibitor of apoptosis protein 1; IκBα: inhibitor κBα; *Ica*: voltage-gated calcium currents; IFN-γ: interferon- γ; IL: interleukin; iNOS: inducible nitric oxide synthase; JAK2: janus kinase 2; LDH: lactate dehydrogenase; MAPKs: mitogen-activated protein kinases; MCP-1: monocyte chemoattractant protein-1; MPO: myeloperoxidase; NF-κB: nuclear factor kappa-light-chain-enhancer of activated B cells; NOD1: nucleotide-binding oligomerization domain-containing protein 1; Nrf2: nuclear factor erythroid 2-related factor 2; Ocln: occludin; OPN: osteopontin; PAI-1: plasminogen activator inhibitor-1; PGE_2: prostaglandin E_2; PI3K: phosphoinositide 3-kinase; PLCγ2: Phospholipase Cγ2; PTEN: phosphatase and tensin homolog; RANKL: receptor activator of NF-κB ligand; RIP-3: receptor interaction protein kinase-3; ROS: reactive oxygen species; Sirt1: sirtuin 1; SOD: superoxide dismutase; STAT3: signal transducer and activator of transcription 3; TGF-β: transforming growth factor-β; TLR4: toll-like receptor 4; TNF-α: tumor necrosis factor α; TRAP: tartrate-resistant acid phosphatase; VAV2: Vav guanine nucleotide exchange factor 2; ZO-1: zonula occluden.

Acknowledgements

Declaration of AI use

During the preparation of this manuscript, the authors used Generative AI (ChatGPT-4) to improve the language, clarity, and readability of the text. The authors critically reviewed and edited all AI-generated suggestions as necessary and take full responsibility for the content of the published article.

Author contributions

N.H.M.: Methodology, Writing – original draft, Writing – review & editing. J.J.: Writing – review & editing. H.A.H.: Resources, Visualization. Y.K.: Writing – review & editing.

Competing Interests

The authors have declared that no competing interest exists.

References

1. Chang WT, Wu SN. Effectiveness of Columbianadin, a Bioactive Coumarin Derivative, in Perturbing Transient and Persistent INa. Int J Mol Sci. 2021;22(2):621.
2. Yang Y, Zhu R, Li J, Yang X, He J, Wang H, et al. Separation and Enrichment of Three Coumarins from Angelicae Pubescentis Radix by Macroporous Resin with Preparative HPLC and Evaluation of Their Anti-Inflammatory Activity. Molecules. 2019;24(14):2664.
3. Zhang C, Hsu AC, Pan H, Gu Y, Zuo X, Dong B, et al. Columbianadin Suppresses Lipopolysaccharide (LPS)-Induced Inflammation and Apoptosis through the NOD1 Pathway. Molecules. 2019;24(3):549.
4. Jayakumar T, Hou SM, Chang CC, Fong TH, Hsia CW, Chen YJ, et al. Columbianadin Dampens In Vitro Inflammatory Actions and Inhibits Liver Injury via Inhibition of NF-κB/MAPKs: Impacts on ·OH Radicals and HO-1 Expression. Antioxidants (Basel). 2021;10(4):553.
5. Wu Y, Hussain SA, Luo M. Columbianadin ameliorates experimental acute reflux esophagitis in rats via suppression of NF-κB pathway. Acta Cir Bras. 2024;39:e391824.
6. Ma Z, Peng L, Sheng Y, Chu W, Fu Y. Anti-Inflammatory Effect of Columbianadin against D-Galactose-Induced Liver Injury In Vivo via the JAK2/STAT3 and JAK2/p38/NF-κB Pathways. Pharmaceuticals (Basel). 2024;17(3):378.
7. Peng B, Rao L, Yang J, Ku X, Kong B, Shuai W, et al. Columbianadin attenuates doxorubicin-induced cardiac injury, oxidative stress, and apoptosis via Sirt1/FOXO1 signaling pathway. Acta Cir Bras. 2023;38:e382223.
8. Bahadır O, Çitoğlu GS, Ozbek H, Dall'Acqua S, Hošek J, Smejkal K. Hepatoprotective and TNF-α inhibitory activity of Zosima absinthifolia extracts and coumarins. Fitoterapia. 2011;82(3):454-9.
9. Niu ZC, An R, Shi HH, Jin Q, Song JL, Chang YX, et al. Columbianadin Ameliorates Myocardial Injury by Inhibiting Autophagy Through the PI3K/Akt/mTOR Signaling Pathway in AMI Mice and Hypoxic H9c2 Cells. Phytother Res. 2025;39(1):521-35.
10. Hou SM, Hsia CW, Tsai CL, Hsia CH, Jayakumar T, Velusamy M, et al. Modulation of human platelet activation and in vivo vascular thrombosis by columbianadin: regulation by integrin αIIbβ3 inside-out but not outside-in signals. J Biomed Sci. 2020;27(1):60.
11. Hsia CW, Yang CH, Sheu JR, Hsia CH, Tsai CL, Huang WC, et al. Reduction of NF-κB Signals in Platelets and Prolongation of Platelet Plug Formation against High Shear Flow in Whole Blood on Human Subject by Columbianadin. Appl Sci (Basel). 2020;10(20):7323.
12. Su X, Wu B, Zhang W, Ji YH, Wang Q, Tan ZY. Inhibitory Effects of Columbianadin on Nociceptive Behaviors in a Neuropathic Pain Model, and on Voltage-Gated Calcium Currents in Dorsal Root Ganglion Neurons in Mice. Front Pharmacol. 2020;10:1522.
13. Kang JI, Hong JY, Choi JS, Lee SK. Columbianadin Inhibits Cell Proliferation by Inducing Apoptosis and Necroptosis in HCT116 Colon Cancer Cells. Biomol Ther (Seoul). 2016;24(3):320-7.
14. Mao S, Xu C, Zou L. Columbianadin Ameliorate Osteoporosis Against Glucocorticoid Induced Osteoporosis in Rats via Alteration of RANK/RANKL/OPG Signaling Pathway. J Biochem Mol Toxicol. 2025;39(8):e70432.
15. Wei Q, Niu ZC, Fu XY, OuYang MH, Guo XT, Li J, et al. S6K/FLNC/ITGβ3 signaling pathway regulates osteoclastogenesis and the inhibition of osteoclastogenesis by columbianadin. Phytomedicine. 2025;136:156276.
16. Rani R, Long S, Pareek A, Dhaka P, Singh A, Kumar P, et al. Multi-target direct-acting SARS-CoV-2 antivirals against the nucleotide-binding pockets of virus-specific proteins. Virology. 2022;577:1-15.
17. Wang Y, Tang L, Miao J, Cheng S, Xu Y, Xie W. Pharmacological and Pharmacokinetic Insights Into Columbianadin: A Promising Natural Anti-Inflammatory Compound. Mediators Inflamm. 2025;2025:6284834.
18. Wang Y, Guan T, Yue X, Yang J, Zhao X, Chang A, et al. The biosynthetic pathway of coumarin and its genetic regulation in response to biotic and abiotic stresses. Front Plant Sci. 2025;16:1599591.
19. Yang L, Hou A, Wang S, Zhang J, Man W, Guo X, et al. A Review of the Botany, Traditional Use, Phytochemistry, Analytical Methods, Pharmacological Effects, and Toxicity of Angelicae Pubescentis Radix. Evid Based Complement Alternat Med. 2020;2020:7460781.
20. Gong S, Wu W, Wang X, Feng S, Zhao J, Fan Y, et al. Enzymatic innovations in Angelica pubescens reveal dual coumarin biosynthetic pathways driving metabolic diversification. Plant J. 2026;125(3):e70707.
21. Zhao Y, Jian X, Wu J, Huang W, Huang C, Luo J, et al. Elucidation of the biosynthesis pathway and heterologous construction of a sustainable route for producing umbelliferone. J Biol Eng. 2019;13:44.
22. Wang K, Zeng H, Dai Y, Wang Z, Tang H, Li J, et al. Three types of enzymes complete the furanocoumarins core skeleton biosynthesis in Angelica sinensis. Phytochemistry. 2024;222:114102.
23. Li J, Li Z, Luo Q, Wang CP, He J, Pang X, et al. Simultaneous Determination of Columbianadin and Its Metabolite Columbianetin in Rat Plasma by LC-MS/MS: Application to Pharmacokinetics of Columbianadin after Oral Administration. Evid Based Complement Alternat Med. 2018;2018:8568303.
24. Zhang YB, Yang XW. Tissue distribution study of columbianadin and its active metabolite columbianetin in rats. Biomed Chromatogr. 2016;30(2):256-62.
25. Yang YF, Zhang L, Yang XW. Distribution Assessments of Coumarins from Angelicae Pubescentis Radix in Rat Cerebrospinal Fluid and Brain by Liquid Chromatography Tandem Mass Spectrometry Analysis. Molecules. 2018;23(1):225.
26. Zoroddu S, Zinellu A, Carru C, Mangoni AA. Neopterin in inflammation and oxidative stress. Adv Clin Chem. 2026;130:61-98.
27. Zhang YB, Li W, Yang XW. Biotransformation of columbianadin by rat hepatic microsomes and inhibition of biotransformation products on NO production in RAW 264.7 cells in vitro. Phytochemistry. 2012;81:109-16.
28. Saxena M, Yeretssian G. NOD-Like Receptors: Master Regulators of Inflammation and Cancer. Front Immunol. 2014;5:327.
29. Lim HJ, Lee JH, Choi JS, Lee SK, Kim YS, Kim HP. Inhibition of airway inflammation by the roots of Angelica decursiva and its constituent, columbianadin. J Ethnopharmacol. 2014;155(2):1353-61.
30. Wu SS, Xu XX, Shi YY, Chen Y, Li YQ, Jiang SQ, et al. System pharmacology analysis to decipher the effect and mechanism of active ingredients combination from herb couple on rheumatoid arthritis in rats. J Ethnopharmacol. 2022;288:114969.
31. Tian T, Wang Z, Zhang J. Pathomechanisms of Oxidative Stress in Inflammatory Bowel Disease and Potential Antioxidant Therapies. Oxid Med Cell Longev. 2017;2017:4535194.
32. Matuz-Mares D, González-Andrade M, Araiza-Villanueva MG, Vilchis-Landeros MM, Vázquez-Meza H. Mitochondrial Calcium: Effects of Its Imbalance in Disease. Antioxidants (Basel). 2022;11(5):801.
33. Yan P, Wang J, Lei Z, Chang H, Shi W, Wang S. The interplay of ferroptosis and oxidative stress in pulmonary fibrosis: from mechanisms to treatment. Front Cell Dev Biol. 2026;14:1709805.
34. Zhang Y, Cao P, Qin D, Zhao Y, Chen X, Ma P. Anti-inflammatory, anti-colitis, and antioxidant effects of columbianadin against DSS-induced ulcerative colitis in rats via alteration of HO-1/Nrf2 and TLR4-NF-κB signaling pathway. Inflammopharmacology. 2025;33(1):341-52.

35. Kazemifard N, Golestani N, Jahankhani K, Farmani M, Ghavami SB. Ulcerative colitis: the healing power of macrophages. Tissue Barriers. 2025;13(2):2390218.
36. Rizo-Téllez SA, Sekheri M, Filep JG. Myeloperoxidase: Regulation of Neutrophil Function and Target for Therapy. Antioxidants (Basel). 2022;11(11):2302.
37. Vajjhala PR, Lu A, Brown DL, Pang SW, Sagulenko V, Sester DP, et al. The Inflammasome Adaptor ASC Induces Procaspase-8 Death Effector Domain Filaments. J Biol Chem. 2015;290(49):29217-30.
38. Kuo WT, Odenwald MA, Turner JR, Zuo L. Tight junction proteins occludin and ZO-1 as regulators of epithelial proliferation and survival. Ann N Y Acad Sci. 2022;1514(1):21-33.
39. Zhang Y, Xi H, Qin D, Cao P, Yang S, Yin J, et al. Construction of a nanozyme composite drug delivery system based on columbianadin for inflammatory bowel disease therapy. RSC Adv. 2026;16(5):4640-54.
40. Xiao S, Wang W, Shi P, He K, Peng C, Zhang Y, et al. Columbianadin improves M1 polarization of microglia after spinal cord injury by stabilizing PTEN and inhibiting the PI3K/AKT pathway. Phytomedicine. 2026;151:157767.
41. Chen S, Wang Y, Zhang L, Han Y, Liang C, Wang S, et al. Therapeutic effects of columbianadin from Angelicae Pubescentis radix on the progression of collagen-induced rheumatoid arthritis by regulating inflammation and oxidative stress. J Ethnopharmacol. 2023;316:116727.
42. Han R, Huang H, Xia W, Liu J, Luo H, Tang J, et al. Perspectives for Forkhead box transcription factors in diabetic cardiomyopathy: Their therapeutic potential and possible effects of salvianolic acids. Front Cardiovasc Med. 2022;9:951597.
43. Delbridge LMD, Mellor KM, Taylor DJ, Gottlieb RA. Myocardial stress and autophagy: mechanisms and potential therapies. Nat Rev Cardiol. 2017;14(7):412-25.
44. Poznyak AV, Kirichenko TV, Beloyartsev DF, Churov AV, Kovyanova TI, Starodubtseva IA, et al. Rheumatoid Arthritis: What Inflammation Do We Face? J Mol Pathol. 2024;5(4):454-65.
45. Gao Y, Zhang Y, Liu X. Rheumatoid arthritis: pathogenesis and therapeutic advances. MedComm (2020). 2024;5(3):e509.
46. Chen S, Bai Y, Wang Y, Liang C, Du K, Wang S, et al. Immunosuppressive effect of Columbianadin on maturation, migration, allogenic T cell stimulation and phagocytosis capacity of TNF-α induced dendritic cells. J Ethnopharmacol. 2022;285:114918.
47. Wang Z, Liu H, Cao Y, Zhang T, Guo H, Wang B. A novel method for investigating the mechanism of the anti-rheumatoid arthritis activity of Angelicae pubescentis radix by integrating UHPLC-QTOF/MS and network pharmacology. Biomed Chromatogr. 2022;36(8):e5389.
48. Han Y, Liu C, Chen S, Sun H, Jia Z, Shi J, et al. Columbianadin ameliorates rheumatoid arthritis by attenuating synoviocyte hyperplasia through targeted vimentin to inhibit the VAV2/Rac-1 signaling pathway. J Adv Res. 2025;74:609-20.
49. Li Z, Huang Z, Liao X, Li H. Columbianadin targets TRIM7 to maintain P2X7 palmitoylation, inhibiting cuproptosis in synovial M2 macrophages. Phytomedicine. 2025;146:157091.
50. Zhao J, Guo S, Schrodi SJ, He D. Cuproptosis and cuproptosis-related genes in rheumatoid arthritis: Implication, prospects, and perspectives. Front Immunol. 2022;13:930278.
51. Liang B, Burley G, Lin S, Shi YC. Osteoporosis pathogenesis and treatment: existing and emerging avenues. Cell Mol Biol Lett. 2022;27(1):72.
52. Kužma M, Jackuliak P, Killinger Z, Payer J. Parathyroid Hormone-Related Changes of Bone Structure. Physiol Res. 2021;70(Suppl 1):S3-S11.
53. Sang Y, Roest M, de Laat B, de Groot PG, Huskens D. Interplay between platelets and coagulation. Blood Rev. 2021;46:100733.
54. Tokarz-Deptuła B, Baraniecki Ł, Palma J, Stosik M, Syrenicz A, Kołacz R, et al. Platelets and Their Role in Immunity: Formation, Activation and Activity, and Biologically Active Substances in Their Granules and Extracellular Vesicles. Int J Inflam. 2025;2025:8878764.
55. Fuentes E, Wehinger S, Trostchansky A. Regulation of Key Antiplatelet Pathways by Bioactive Compounds with Minimal Bleeding Risk. Int J Mol Sci. 2021;22(22):12380.
56. Dho SH, Cho M, Woo W, Jeong S, Kim LK. Caspases as master regulators of programmed cell death: apoptosis, pyroptosis and beyond. Exp Mol Med. 2025;57(6):1121-32.
57. Czabotar PE, Lessene G, Strasser A, Adams JM. Control of apoptosis by the BCL-2 protein family: implications for physiology and therapy. Nat Rev Mol Cell Biol. 2014;15(1):49-63.
58. Fukai T, Ushio-Fukai M. Superoxide dismutases: role in redox signaling, vascular function, and diseases. Antioxid Redox Signal. 2011;15(6):1583-606.
59. Schieber M, Chandel NS. ROS function in redox signaling and oxidative stress. Curr Biol. 2014;24(10):R453-62.
60. Zhang W, Dong J, Xu J, Qian Y, Chen D, Fan Z, et al. Columbianadin suppresses glioblastoma progression by inhibiting the PI3K-Akt signaling pathway. Biochem Pharmacol. 2024;223:116112.
61. Chen S, Li L. Degradation strategy of cyclin D1 in cancer cells and the potential clinical application. Front Oncol. 2022;12:949688.
62. Kocot-Kępska M, Zajączkowska R, Mika J, Wordliczek J, Dobrogowski J, Przeklasa-Muszyńska A. Peripheral Mechanisms of Neuropathic Pain-the Role of Neuronal and Non-Neuronal Interactions and Their Implications for Topical Treatment of Neuropathic Pain. Pharmaceuticals (Basel). 2021;14(2):77.
63. Lolignier S, Eijkelkamp N, Wood JN. Mechanical allodynia. Pflugers Arch. 2015;467(1):133-9.
64. Cohen SP, Mao J. Neuropathic pain: mechanisms and their clinical implications. BMJ. 2014;348:f7656.
65. Ton FN, Gunawardene SC, Lee H, Neer RM. Effects of low-dose prednisone on bone metabolism. J Bone Miner Res. 2005;20(3):464-70.
66. Rauch A, Seitz S, Baschant U, Schilling AF, Illing A, Stride B, et al. Glucocorticoids suppress bone formation by attenuating osteoblast differentiation via the monomeric glucocorticoid receptor. Cell Metab. 2010;11(6):517-31.